AD_____

Award Number: W81XWH-04-2-0027

TITLE: Creation of Polyvalent Decoys of Protein Cytotoxins as Therapeutics and Vaccines

PRINCIPAL INVESTIGATOR: Vijay S. Reddy, Ph.D.

CONTRACTING ORGANIZATION: The Scripps Research Institute
La Jolla, CA 92037

REPORT DATE: January 2008

TYPE OF REPORT: Final

PREPARED FOR: U.S. Army Medical Research and Materiel Command
Fort Detrick, Maryland 21702-5012

REPORT DOCUMENTATION PAGE

Form Approved
OMB No. 0704-0188

1. REPORT DATE *(DD-MM-YYYY)*	**2. REPORT TYPE**	**3. DATES COVERED** *(From - To)*
01-01-2008	Final	15 JUL 2004 - 31 DEC 2007

4. TITLE AND SUBTITLE

Creation of Polyvalent Decoys of Protein Cytotoxins as Therapeutics and Vaccines

5a. CONTRACT NUMBER

5b. GRANT NUMBER
W81XWH-04-2-0027

5c. PROGRAM ELEMENT NUMBER

6. AUTHOR(S)
Vijay S. Reddy, Ph.D.

E-Mail: reddyv@scripps.edu

5d. PROJECT NUMBER

5e. TASK NUMBER

5f. WORK UNIT NUMBER

7. PERFORMING ORGANIZATION NAME(S) AND ADDRESS(ES)

The Scripps Research Institute
La Jolla, CA 92037

8. PERFORMING ORGANIZATION REPORT NUMBER

9. SPONSORING / MONITORING AGENCY NAME(S) AND ADDRESS(ES)
U.S. Army Medical Research and Materiel Command
Fort Detrick, Maryland 21702-5012

10. SPONSOR/MONITOR'S ACRONYM(S)

11. SPONSOR/MONITOR'S REPORT NUMBER(S)

12. DISTRIBUTION / AVAILABILITY STATEMENT
Approved for Public Release; Distribution Unlimited

13. SUPPLEMENTARY NOTES

14. ABSTRACT

Polyvalent protein shells (capsids) are useful platforms for the display of molecules of interest (MOI) on their surface. The resultingpolyvalent reagents can be used as efficacious prophylactic vaccines and therapeutics. The coat protein subunits of Tomato Bushy StuntVirus (TBSV) and structurally similar Norwalk viruses, when expressed in insect cells, spontaneously self assemble to form proteinshells. The self-assembly of the coat protein mutants of TBSV resulted in two types of nanoparticles: small (60 subunit) and the regularsize (180 subunit) capsids. Norwalk virus particles predominantly result in formation of 180 subunit shells. These protein shells(capsids) can be used for the display of 60-180 copies of peptides/proteins of the pathogens of concern.Previously, it has been shown that antibodies raised against various cytotoxins (e.g., ricin and Shiga toxin) render protection against thepotential toxin attack. The proposed polyvalent reagents, which display various peptide/protein fragments of ricin would act asefficacious prophylactic vaccines of the ricin toxin by priming the immune system. We have successfully produced two polyvalentreagents displaying multiple copies of 1) 16 a.a. RTA antigenic peptide (mouse epitope) and 2) a large 188 a.a. stable RTA domain.

15. SUBJECT TERMS
Stress, cerebral bloodflow, performance, vigilance, sustained attention, fatigue, vehicle driving, individual differences, workload

16. SECURITY CLASSIFICATION OF:			**17. LIMITATION OF ABSTRACT**	**18. NUMBER OF PAGES**	**19a. NAME OF RESPONSIBLE PERSON**
					USAMRMC
a. REPORT	**b. ABSTRACT**	**c. THIS PAGE**			**19b. TELEPHONE NUMBER** *(include area code)*
U	U	U	UU	29	

Standard Form 298 (Rev. 8-98)
Prescribed by ANSI Std. Z39.18

Table of contents:

INTRODUCTION & SUMMARY

The proposal titled "Creation of Polyvalent Decoys of Protein Cytotoxins as Therapeutics and Vaccines" entails displaying multiple (60-180) copies of antigenic regions of varying lengths (1-200a.a.) of the cytotoxins, ricin in particular, on the surface of viral capsids (protein shells). These polyvalent reagents (PVRs) have been shown to be efficacious prophylactic vaccines and/or inhibitors of the corresponding toxins, if PVRs could be used display the Fabs of ricin antibodies (Mourez et al., 2001). In this regard, we have created the protein shells of Tomato Bushy Stunt Virus (TBSV) and Norwalk viruses (Sinsiro and Seto) by over-expressing the respective coat proteins (CPs) that self-assemble to form homogenous capsids composed of 60/180 CP subunits. The first step of generating the two different types of protein shells was clearly accomplished. The 2-domain (S and P) organization of the coat protein subunits of these capsids facilitate the display of any proteins/peptides of interest either by replacing the C-terminal P-domains of the coat protein subunits or appending at the end of the P-domain. We have used these protein shells (e.g., TBSV) to generate PVRs as decoys of cytotoxins by appending the antigenic epitopes of cytotoxins at the end of the P-domain of the TBSV capsid protein. These PVRs, when injected in mice, resulted in the induction of antibodies, thus perhaps providing the passive immunity against the cytotoxins.

BODY OF REPORT

STATEMENT OF WORK:

Expression and structural characterization of the polyvalent display platform of altered (mutant) capsids of Tomato Bushy Stunt Virus (TBSV) and Norwalk Viruses.

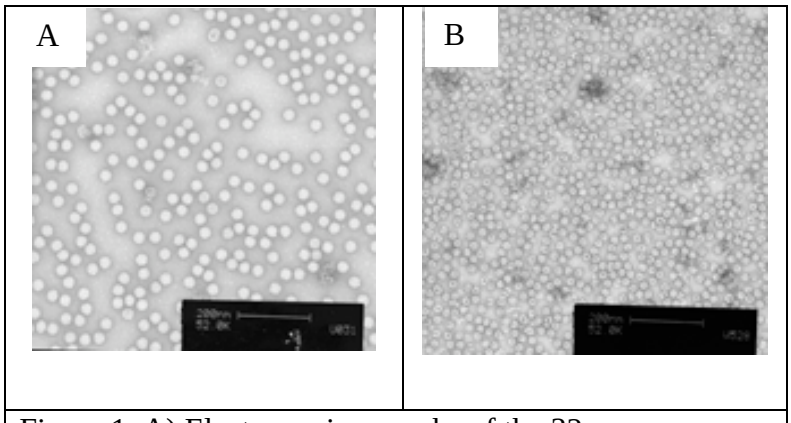

Figure 1. A) Electron micrographs of the 32nm nanoparticles (protein shells) assembled from the full-length TBSV coat protein. B) Smaller 21nm nanoparticles assembled from the coat protein (CP-NΔ72) with the first 72 amino acids deleted. All the samples were visualized by coating with 1% uranyl aceate stain.

Generation of protein shells of TBSV capsid proteins in insect cells:

The capsid protein subunits of TBSV have been expressed in insect cells successfully using baculovirus system. Full length (CP-FL) and a N-terminal deletion mutant (CP-NΔ52) of the TBSV capsid protein form native like (T=3) protein shells of 32nm in diameter made up of 180 protein subunits, while the longer N-terminal deletion mutants, CP-NΔ72 and CP-

NΔ82 from smaller 21nm diameter (T=1) particles with 60 subunits (Figure 1; Hsu et al., 2006).

Cryo-electron microcopy and image reconstruction methods were employed to determine the structures of respective particles at about 20Å resolution (Figure 2). The above results suggest that each kind of the protein shells were made uniformly with high fidelity.

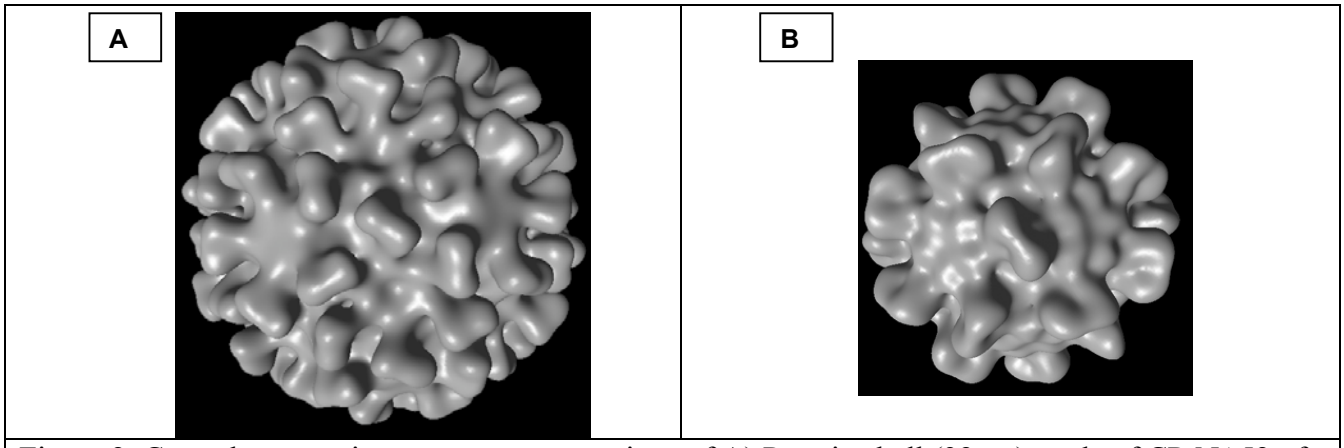

Figure 2. Cryo electron microscopy reconstructions of A) Protein shell (32nm) made of CP-NΔ52 of TBSV B) Smaller (21nm) particles made of TBSV CP-NΔ72.

Generation of protein shells of Norwalkvirus capsid proteins in insect cells:

Like many Norovirus VLPs in the literature, we have successfully generated native VLPs of Sinsiro virus and Seto virus VLPs (Kobayashi et al., 2000b; Kumar et al., 2007). Seto virus and Sinsiro viruses belong to the Genogroups I and II respectively with 47% sequence similarity. Figure 3 shows the SDS page gel, Western blot and micrographs corresponding to the VLPs of Seto and Sinsiro viruses. The recombinant baculoviruses expressing these CPs were generated and expressed in Sf21 cells.

In addition, we have recently characterized the unique trypsinization observed, for the first time, in the assembled Norovirus (Sinsiro virus (SV)) particles, employing the N-terminal sequencing, MALDI-TOF and Western blot analysis (Kumar et al., 2007). Previously, it was shown that the GI group viruses are not susceptible for trypsinization in the assembled form. However, GI viruses as well as GII viruses undergo trypsinization when the particles are disassembled into soluble coat proteins (Hardy et al., 1995). The trypsinization of the VLPs of Sinsiro virus (SV), a G-II virus, in the assembled form is due to a 20 a.a. insertion (297-316) with a basic amino acid (R307) present in the surface exposed P2 domain of the Sinsiro virus. Interestingly, the SV particles remain assembled even after the trypsinization. The 20 a.a. insertion is seen only in subgroups 3 and 6 of the Genogroup II. Figure 3F shows the multiple sequence alignment of the P2 domains of various strains of NoVs in the region of the 20 a.a. insertion.

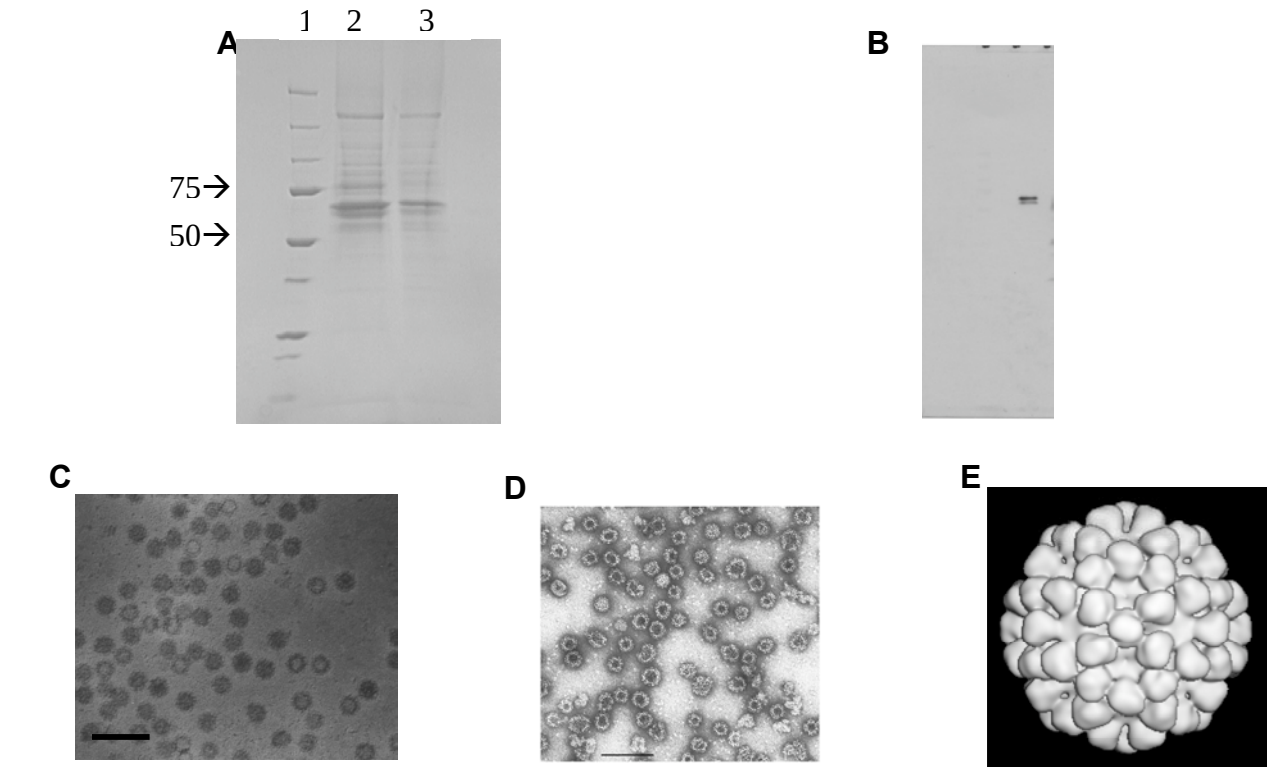

F

```
Norwalk        (G1_1) 291 RGTSNGTVIN--------------------LTELDG...... SARGRLGLRR 530
Msham-Gbr95    (G2_2) 287 KGEVTAHLHDNDH------------LNNVTITNLNG...... GRRRVQ---- 542
Hilingd-GBR00  (G2_5) 287 RGKVTGQFPNEQN------------MWNLEITNLNG...... GRRRFQ---- 540
Erfurt-DEU01   (G2_10)287 RGKVTQQVQDEHRG----------THWNMTVTNLNG...... GRRRMQ---- 548
Hawaii-USA91   (G2_1) 287 RGRINAQVPDDHH------------QWNLQVTNTNG...... GRRRVQ---- 535
Amstdam-NLD99  (G2_8) 287 RGTLQTR-----------LADQPNYTYQVHLENLDG...... GRRRVQ---- 537
VABeach-USA01  (G2_9) 287 KGTLQAE-----------VPG-QHQLYQLQLTNLDG...... GRRRIQ---- 537
Leeds-GBR00    (G2_7) 287 KGEVIAK-----------NGDVRSYRMDMEITNTDG...... GRRRVQ---- 540
Toronto-CAN93  (G2_3) 287 RGTLTRSTSRASDQADTPTPRLFNYYWHIQLDNLNG...... GRRRIQ---- 548
Sinsiro        (G2_3) 287 RGVLTRSTSRASDQADTATPRLFNYYWHVQLDNLNG...... GRRRIQ---- 548
Seacrof-GBR00  (G2_6) 286 RGTLISQTARAADSTDSPQ-RARNHPLHVQVKNLDG...... GRRRAQ---- 550
Bristol-GBR93  (G2_4) 287 RGDVTHIAG-------------SHDYTMNLASQNW...... GRRRAL---- 539
VA387          (G2_4) 287 RGDVTHIAG-------------SHDYIMNLASQNW...... GRRRAL---- 539
```

Figure 3. Gels and micrographs of Seto and Sinsiro virus VLPs. A) SDS page gel of showing the ~60kDa CP of two NoVs. Lanes 1) MW marker 2) Seto Virus CP 3) Sinsiro Virus (SV) CP. B) Western blot using the SV antibodies detects only sinsiro virus CP. Electron micrographs showing C) Negative stained particles of Seto virus D) Sinsiro virus. E) Image reconstruction at 30Å resolution of the Sinsiro virus VLPs generated based on the negatively stained particles seen in the panel D. F) Sequence alignment of the P2 domains of various members of both GI and GII NoVs in the region of 20a.a. insertion in the Sinsiro Virus P2 domain.

The peptide of residues (325-334) in SV, corresponding to the linear epitope suggested to be responsible for host cell interactions in Snow Mountain virus (Lochridge et al., 2005), remains contiguous even after the SV particles undergo trypsinization. We hypothesized that the proteolytic cleavage of the SV capsids renders the linear epitope free and exposed, but still tethered to the assembled capsid, thereby enhancing the ability of the virus to bind to susceptible host cells (Kumar

et al., 2007). This perhaps could be the reason for the greater virulence of Sinsiro virus and other GII.3 NoVs in general. The highly exposed loop (297-316) could replaced with a peptide epitope of interest to generate Norwalk virus based PVRs.

Creation of polyvalent reagents (decoys) of ricin toxin by displaying RTA epitopes on TBSV capsids:

Due to instability of the resulting protein shells of the Sinsiro virus, the TBSV capsids were chosen as the preferred display platforms for generating the polyvalent reagents. Having successfully generated two sizes of TBSV nanoparticles (protein shells) as display plat forms, the first polyvalent reagent (TBSV-RTA16) was created by genetically appending an epitope of residues 95-110 of the ricin A-chain at the C-terminal end of the TBSV coat protein. It has been shown that the above epitope of the ricin-A chain generates neutralizing antibodies that render protection against the ricin toxin (Olson et al., 2004). This novel reagent contains 180 copies of the RTA peptide displayed on the surface of TBSV capsid.

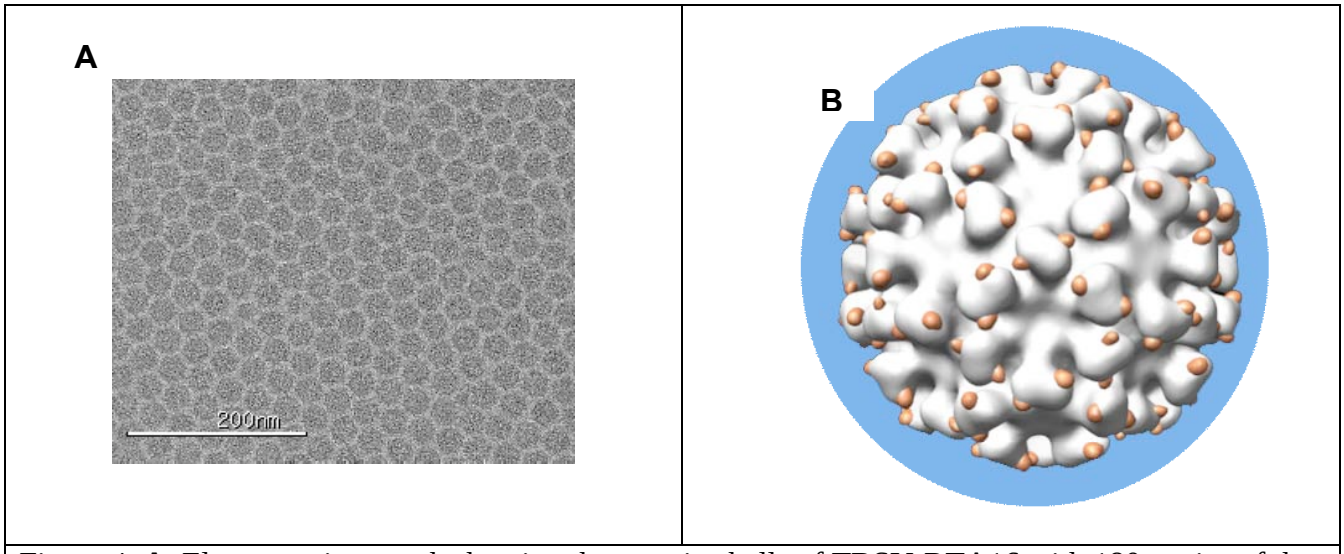

Figure 4. **A.** Electron micrograph showing the protein shells of TBSV-RTA16 with 180 copies of the RTA peptide of residues 95-110 displayed on its surface. **B.** Cryo-EM reconstruction of TBSV-RTA16 reagent (vaccine) showing the highly exposed epitopes (in gold) of the ricin toxin.

Figure 4 shows an electron micrograph and the cryo-EM reconstruction of the TBSV-RTA16 reagent. Highly exposed ricin epitopes makes it an highly efficient reagent in producing antibodies, which detect the ricin toxin. Figure 5 shows the results that illustrate the ability of the antibodies generated in mice by the above PVR in detecting the ricin toxin. These antibodies detect the parent reagent (TBSV-RTA16) as well as the ricin toxin in the western-blot analyses. The size of the TBSV-RTA16 subunit is ~38kDa and are identified by the asterisks. Higher and lower size bands in the same lanes

correspond to the multimers and cleavage products of the subunits respectively. Not surprisingly, only the ricin A-chain is detected by the antibodies due to the TBSV-RTA16 reagent. This proves that the basic methodology works in generating the antibodies, which provide protection against the ricin toxin without causing any toxic effects. These polyvalent reagents (PVRs) will be highly efficacious compared to single molecules/peptides on molar basis in generating antibodies against the ricin, hence provide greater protection against the toxin attack. Efficacy of the antibodies in providing protection against the ricin-toxin using the cell-intoxication experiments will be tested in future.

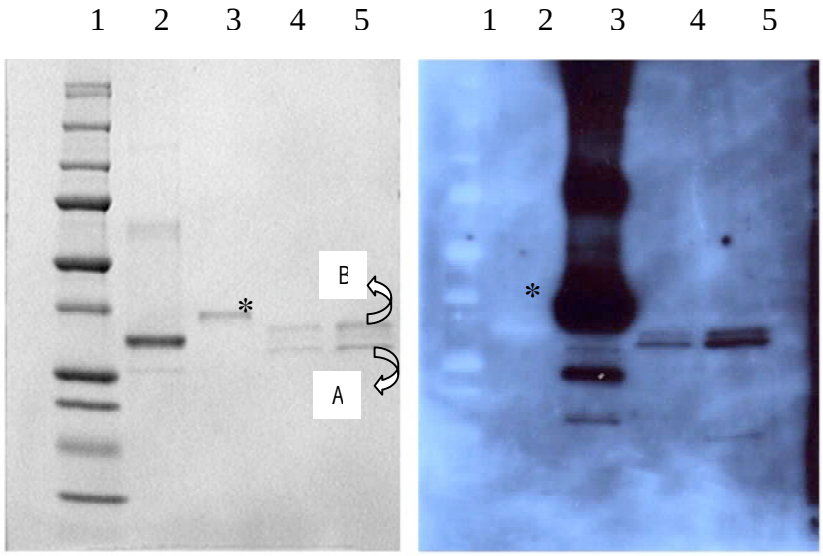

Figure 5. Detection of ricin toxin by the antibodies due to TBSV-RTA16 displaying ricin epitope. Shown on the left is the SDS page and on the right is the western blot of the proteins Lanes **1**. M.W. markers, **2**. TBSV-Δ72 (netative control), **3**. TBSV-RTA16, **4**. Ricinus communis agglutinin (RCA) as positive control. A and B chains are identified by the curled arrows, while the TBSV-RTA16 bands are identified by an asterisk.

We recently generated a new PVR that displays multiple copies of the stable RTA domain of 188 a.a., which by itself has been proven to be a potential vaccine candidate (Olson et al., 2004). This new reagent, namely TBSV-RTA188, was generated by appending the RTA188 domain at the end of the TBSV-subunit.

Figure 6 shows the EM micrograph and a western blot analysis of the new reagent along with the TBSV-RTA16 detected using commercially available ricin antibodies. The size of the newly generated chimeric protein of TBSV-RTA188 is ~60kDa, identified by an asterisk (Figure 6B). Higher bands correspond to higher oligomers of the chimeric protein. This particular PVR appear to form smaller particles and perhaps they may contain 60 copies of the RTA domains. The actual number of RTA domains present in this PVR is currently under investigation. Recent preparations of the TBSV-RTA188 reagent resulted in a lot of broken particles, suggesting that instability of these protein shells due to over crowding the RTA domains there by interfering with the particle assembly. Display of the RTA188 domain on smaller TBSV and or Norwalk virus particles will be explored if any funding becomes available in near future.

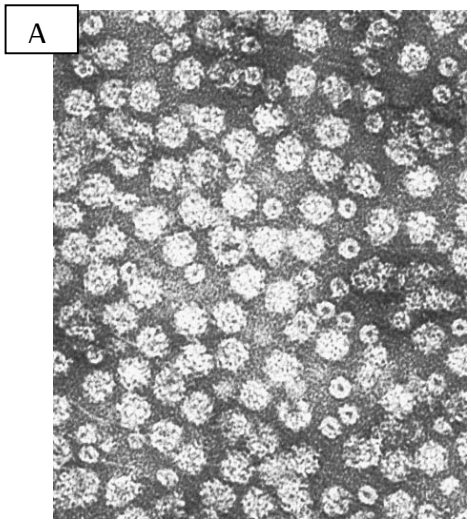

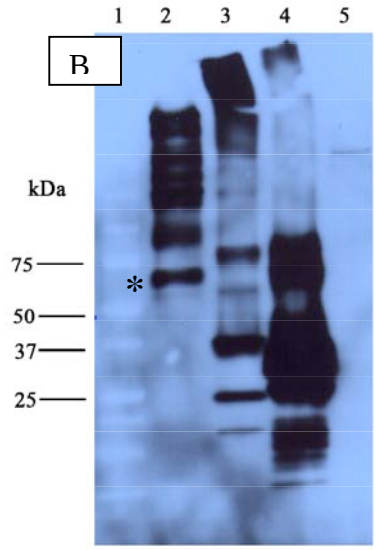

Figure 6. A. Electron micrograph of TBSV-RTA188 polyvalent reagent. Larger particles in the micrograph correspond to the TBSV-RTA188. The identity of the smaller particles is under investigation. B. Western blot analysis of the TBSV-RTA188 reagent. Lanes 1) M.W. Markers, 2) TBSV-RTA188, 3) TBSV-RTA16, 4) purified ricin toxin, 5) TBSV-Δ72 as the negative control.

KEY RESEARCH ACCOMPLISHMENTS:

1) Expression/Creation of two sizes (21nm, 32nm) of nanoparticles of TBSV capsid proteins using baculovirus system as potential display platforms for the presentation of molecules of interest by genetic modification (Resulted in a publication).
2) Creation of another nanoparticle platform using Norwalk virus (Sinsiro virus and Seto virus) capsid protein using the baculovirus system. Characterization of the unique trypsin cleavage in the assembled Sinsiro virus capsids (Resulted in a publication).
3) Structural characterization of the above nanoparticles using cryo-electron microscopy and image analysis (To be published).
4) Creation and characterization of polyvalent reagent (PVR), the first decoy of ricin toxin, displaying the 180 copies of the RTA peptide of residues 95-110 as a prophylactic ricin vaccine. Antibodies generated in mice using this PVR detect the native ricin toxin. Cryo-EM structural characterization of this PVR reveals the highly exposed disposition of the ricin epitopes, which is highly advantageous for efficacious vaccine (To be published).
5) Creation of a new PVR that displays multiple copies of a larger (188a.a.) and stable RTA domain. These PVRs displaying 180 copies of RTA-188 domains appear to be unstable perhaps due to over crowding. Generation of smaller nanoparticles displaying 60 copies of the RTA188 will be attempted in future (To be published).

CONCLUSIONS:

We have made a number of important advances in the past 3 years by generating platforms for producing polyvalent reagents (PVRs) and creating the decoys of ricin toxin as vaccines and therapeutics. We have created two PVRs: 1) TBSV-RTA16 and 2) TBSV-RTA188, which have shown promise to be potentially useful vaccine candidates, by inducing antibodies that can detect ricin toxin. Further work needs to be done to mature these reagents to be used in animal studies. This technology can be further developed and enhanced to create the best possible vaccines for all the cytotoxins. We will be happy to assist USAMRIID to create such vaccines if funding becomes available in future.

REFERENCES:

Hardy, M. E., White, L. J., Ball, J. M., and Estes, M. K. (1995). Specific proteolytic cleavage of recombinant Norwalk virus capsid protein. *J Virol* 69(3), 1693-8.

Hsu, C., Singh, P., Ochoa, W., Manayani, D. J., Manchester, M., Schneemann, A., and Reddy, V. S. (2006). Characterization of polymorphism displayed by the coat protein mutants of tomato bushy stunt virus. *Virology* **349**(1)**,** 222-9.

Kobayashi, S., Sakae, K., Suzuki, Y., Shinozaki, K., Okada, M., Ishiko, H., Kamata, K., Suzuki, K., Natori, K., Miyamura, T., and Takeda, N. (2000b). Molecular cloning, expression, and antigenicity of Seto virus belonging to genogroup I Norwalk-like viruses. *J Clin Microbiol* **38**(9)**,** 3492-4.

Kumar, S., Ochoa, W., Kobayashi, S., and Reddy, V. S. (2007). Presence of a surface-exposed loop facilitates trypsinization of particles of Sinsiro virus, a genogroup II.3 norovirus. *J Virol* 81(3), 1119-28.

Lochridge, V. P., Jutila, K. L., Graff, J. W., and Hardy, M. E. (2005). Epitopes in the P2 domain of norovirus VP1 recognized by monoclonal antibodies that block cell interactions. *J Gen Virol* 86(Pt 10), 2799-806.

Mourez, M., Kane, R. S., Mogridge, J., Metallo, S., Deschatelets, P., Sellman, B. R., Whitesides, G. M., and Collier, R. J. (2001). Designing a polyvalent inhibitor of anthrax toxin. Nat Biotechnol 19(10), 958-61.

Olson, M. A., Carra, J. H., Roxas-Duncan, V., Wannemacher, R. W., Smith, L. A., and Millard, C. B. (2004). Finding a new vaccine in the ricin protein fold. Protein Eng Des Sel 17(4), 391-7. Epub 2004 Jun 08.

APPENDIX: Publications from W81XWH-04-2-0027

Available online at www.sciencedirect.com
SCIENCE DIRECT
Virology 349 (2006) 222–229
VIROLOGY
www.elsevier.com/locate/yviro

Characterization of polymorphism displayed by the coat protein mutants of tomato bushy stunt virus

Catherine Hsu [a], Pratik Singh [b], Wendy Ochoa [a], Darly J. Manayani [a], Marianne Manchester [b], Anette Schneemann [a], Vijay S. Reddy [a,*]

[a] Department of Molecular Biology, The Scripps Research Institute, 10550 North Torrey Pines Road, La Jolla, CA 92037, USA
[b] Department of Cell Biology, The Scripps Research Institute, 10550 North Torrey Pines Road, La Jolla, CA 92037, USA

Received 26 October 2005; returned to author for revision 22 February 2006; accepted 27 February 2006
Available online 5 April 2006

Abstract

Expression of full-length and N-terminal deletion mutants of the coat protein (CP) of tomato bushy stunt virus (TBSV) using the recombinant baculovirus system resulted in spontaneously assembled virus-like particles (VLPs). Deletion of the majority of the R-domain sequence of the CP, residues 1–52 (CP-NΔ52) and 1–62 (CP-NΔ62), produced capsids similar to wild-type VLPs. Interestingly, the CP-NΔ62 mutant that retains the last 3 residues of R-domain is capable of forming both the T = 1 and T = 3 particles. However, between the two types of VLPs, formation of the T = 1 capsids appears to be preferred. Another mutant, CP-NΔ72, in which R-domain (residues 1–65) was completely removed but contains most of the β-annulus and extended arm (βA) regions exclusively formed T = 1 particles. These results suggest that as few as 3 residues (63–65) of the R-domain, which includes 2 basic amino acids together with the arm (βA) and β-annulus regions, may be sufficient for the formation of T = 3 particles. However, anywhere between 4 to 13 residues of the R-domain may be required for proper positioning of βA and β-annulus structural elements of the C-type subunits to facilitate an error free assembly of T = 3 capsids.

Keywords: Polymorphism; Virus-structure; Tombusviridae; Protein expression; Self assembly

Introduction

Tomato bushy stunt virus (TBSV) is a ~34 nm spherical plant virus that belongs to the family of Tombusviridae. Wild-type TBSV possesses a single positive-sense RNA genome of 4776 bases encapsidated into a capsid with T = 3 icosahedral symmetry, which is made of 180 copies of a single coat protein (CP) subunit of 41 kDa (Harrison et al., 1978; Olson et al., 1983). The genome of TBSV (cherry strain) was sequenced and the cDNA clones of the CP gene were generated (Hearne et al., 1990; Hillman et al., 1989). TBSV and structurally similar turnip crinkle virus (TCV) have been the subjects of structural analysis for a long period of time (Crowther and Amos, 1971; Harrison, 1971; Harrison et al., 1978; Hogle et al., 1986; Olson et al., 1983; Sorger et al., 1986; Stockley et al., 1986). The three-dimensional structures of TBSV and TCV capsids are available at high resolution (Harrison et al., 1978; Hogle et al., 1986; Olson et al., 1983). Fig. 1A shows the quaternary organization of the CP-subunits of TBSV in T = 3 capsids. The tertiary structure of the CP-subunit (Fig. 1B) is composed of three major domains: (1) the R- (RNA binding) domain, formed by the N-terminal residues (1–65) that are disordered in all the subunits, followed by the β-annulus region (residues 67–85) and an "extended arm" of residues 86-101, which are ordered only in the C-type (green) subunits (Fig. 1A); (2) the middle S- (shell) domain, a canonical β-barrel motif comprises of residues 102–268 that forms the contiguous shell of the capsid and (3) the C-terminal P- (projection) domain, made up of residues 273–388 (Figs. 1B and C). The S and P-domains are connected to each other by a four-residue hinge (269–272) (Hogle et al., 1986; Olson et al., 1983; Sorger et al., 1986).

It was shown that, in the case of turnip crinkle virus (TCV), treatment of the disassembled CP-dimers with chymotrypsin and subsequent reassembly of the proteolyzed dimers resulted in the formation of smaller (T = 1) particles (Sorger et al., 1986).

* Corresponding author. Fax: +1 858 784 8688.
E-mail address: reddyv@scripps.edu (V.S. Reddy).

0042-6822/$ - see front matter © 2006 Elsevier Inc. All rights reserved.
doi:10.1016/j.virol.2006.02.038

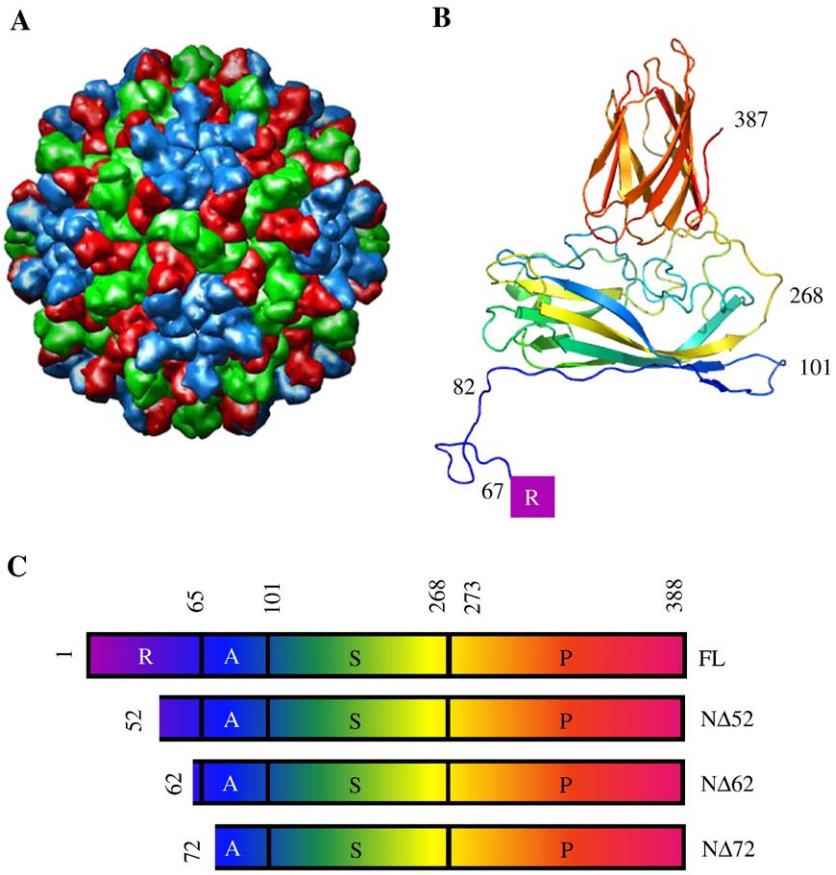

Fig. 1. Illustrations of TBSV structure and the constructions of CP deletion mutants. (A) Quaternary structure of TBSV showing the organization of (180) subunits occupying the 3 different environments (blue, red and green) in the capsid. These three color-coded environments are also commonly referred to as A (blue), B (red) and C (green) type subunits. This figure was obtained from a viral structural database, URL: http://viperdb.scripps.edu (Shepherd et al., 2006). This was generated using the program Chimera (Pettersen et al., 2004). (B) Tertiary structure (ribbon diagram) of the subunits that occupy the green (C-type) locations. A continuous color gradient (rainbow) was employed to identify different regions of the protein. Irrespective of their locations in the capsid: blue (A)/ red (B)/ green (C), the tertiary structures of all the individual subunits are nearly identical with the exception of part of the R-domain (1–65), conserved β-annulus (81–84) residues and Arm (A) (85–100) regions. Residues 1–66 are disordered in all the subunits while the residues 67–100 are selectively ordered in green (C-type) subunits. The figure was generated using the coordinates in the PDB (ID: 2TBV). This figure was generated using the program PyMol (DeLano, 2002). (C) Bar diagrams illustrating different N-terminal deletion mutants prepared and investigated in this study.

The above proteolytic cleavage at the residue 66 of the TCV-CP removed the entire R-domain and parts of the β-annulus regions from the rest of the TCV-CP subunit (Fig. 5). Hence, these regions were suggested to be responsible for forming T = 3 capsids. Even though the coat proteins of TBSV and TCV have only 21% amino acid sequence identity, they display similar subunit structure and particle (T = 3) architecture (Hogle et al., 1986). Because of this structural homology, a similar behavior of particle polymorphism was suggested for TBSV. Although the TBSV-CP gene has been manipulated in order to generate various phenotypes in plants (Hearne et al., 1990; Joelson et al., 1997; Scholthof et al., 1993), there are no reports to date on expression of the TBSV-CP gene in a heterologous expression system.

In this study, we describe the successful expression and spontaneous assembly of virus-like particles (VLPs) from the full-length and various N-terminal deletion mutants of the TBSV CP in insect cells using the baculovirus system. Furthermore, we characterized the polymorphism displayed by the N-terminal deletion mutants, in which different lengths of the R-domain and the β-annulus regions were removed. Generation of TBSV-VLPs has important advantages such as ease of exploring structure–function–assembly relationships and exploiting potential use of the VLPs as display platforms for multivalent presentation of foreign epitopes (Joelson et al., 1997).

Results and discussion

Varying lengths of TBSV-CP gene constructs were expressed in insect cells using the baculovirus expression system, and the formation of VLPs was investigated. The cDNA of the CP (p41) spanning nucleotides 2652–3815, 2805–3815, 2835–3815 and 2865–3815 corresponding to a full-length, 1–388 AA (CP-FL) and N-terminal deletion mutants 53–388 AA (CP-NΔ52), 63–388 AA (CP-NΔ62) and 73–388 AA (CP-NΔ72), respectively, were subcloned each into separate transfer vectors. The recombinant baculovirus constructs were generated using standard procedures (see Materials and methods). *Sf*-21 insect

cells infected with the respective recombinant baculovirus were lysed 3 days post-infection to harvest and analyze the expressed protein. Mock-infected and recombinant-infected cell lysates were first examined using a dot blot assay for the expression of TBSV coat protein. Cell lysates infected with each of the baculovirus constructs showed positive immunoblots indicating expression of the TBSV-CP, while the uninfected cell lysates (negative control) did not react (data not shown). Following confirmation of the expressed protein, the clarified cell lysates were subjected to ultracentrifugation through a 30% sucrose cushion. The pellets containing the partially purified VLPs were resuspended and further purified by ultracentrifugation through 10–40% sucrose gradients. Presence of faint bands visible near the middle of the gradients further confirmed the formation of VLPs. Fractionation of the gradients with continuous monitoring of absorbance at 254 nm revealed a single major peak, discounting the peak at the top of the gradient which corresponds to unassembled soluble protein and with the exception of CP-NΔ62 mutant preparation, which showed two peaks, indicating the formation of two populations of VLPs (Fig. 2A). The faster sedimenting peak nearly coincided with that of peaks from CP-FL and CP-NΔ52 preparations, while the slower sedimenting peak coincided with that of the CP-NΔ72.

SDS PAGE analysis of the purified VLPs showed that each capsid contained a single type of CP subunit (Fig. 2B). Relative to molecular mass standards, the approximate estimated masses of the expressed CP-FL, CP-NΔ52, CP-NΔ62 and CP-NΔ72 proteins were 41 kDa, 36 kDa, 35 kDa and 34 kDa, respectively. Interestingly, the antibodies raised against the wild-type TBSV failed to detect the denatured TBSV-CPs from the purified VLPs in a Western blot assay (data not shown). However, they detected the non-denatured (intact) TBSV VLPs in the dot blot assays indicating that the antibodies react with the conformational epitopes of intact TBSV capsids. Furthermore, a similar pattern was observed when antibodies raised in mice against the purified TBSV-VLPs were used. The mouse anti-TBSV antibodies did not recognize denatured TBSV antigens but reacted very strongly with native antigens in ELISA (Fig. 2C). This further confirmed that the TBSV-VLPs presumably induce only conformational antibodies. We came to know that this type of immune response is not so uncommon after we realized that the TBSV antibodies were ineffective in detecting denatured coat protein. For example, expression of human polyomavirus by recombinant baculovirus system resulted in VLPs that were able to induce only conformational antibodies when injected into rabbits. Both human and rabbit virus-specific antibodies failed to react with denatured viral antigens in dot blot and ELISA (Li et al., 2003). Joelson et al. (1997) utilized antibodies produced by hyper-immunization of rabbits with denatured TBSV particles in order to detect the chimeric virus particles displaying human immunodeficiency virus epitopes in Western blots.

Electron microscopy of negatively stained samples taken from the respective peaks (Fig. 2A) showed the presence of assembled VLPs (Figs. 3A–E). Particles formed by the CP-FL, CP-NΔ52 and the larger capsids of the CP-NΔ62 construct, have an average diameter of ~34 nm (Figs. 3A–C) consistent with the wild-type T = 3 particles of TBSV (Harrison et al., 1978;

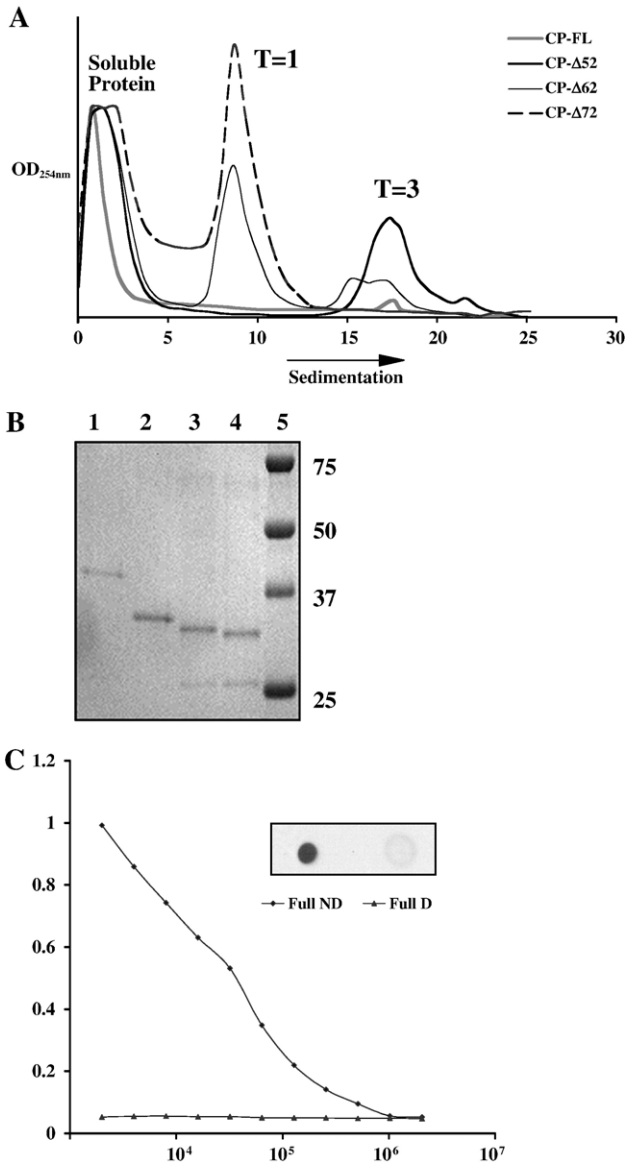

Fig. 2. Biophysical and biochemical characterization of the VLPs of TBSV. (A) Plot showing the UV absorbance profiles of CP-FL, CP-NΔ52 and CP-NΔ62 and CP-NΔ72 is shown. (B) SDS-PAGE analyses of TBSV-VLPs showing the Mr of the corresponding CP-subunits, lanes 1: CP-FL, 2: CP-NΔ52, 3: CP-NΔ62, 4: CP-NΔ72 and 5: molecular weight markers. Tris-Glycine (10–20%) gels (Invitrogen, Carlsbad, CA) were used for all the SDS-PAGE analysis. (C) ELISA assay showing the selective detection of non-denatured coat proteins (●) by the mouse anti-TBSV antibodies over denatured coat protein (▲). Inset shows the corresponding dot blot. In both cases, antigens of CP-FL VLPs were used.

Olson et al., 1983). The smaller particles, ~21 nm in diameter, generated by the CP-NΔ62 and CP-NΔ72 proteins most likely correspond to T = 1 particles. Even though, the CP-NΔ62 forms both types of particles, the formation of the T = 1 particles appears to be more efficient than that of the T = 3 capsids. Similar kinds of smaller (T = 1) particles were obtained earlier by the proteolysis and subsequent reassembly of subunit dimers of turnip crinkle virus (TCV), which is structurally analogous to TBSV (Sorger et al., 1986). TEM examination suggested that a majority of VLPs were not empty (Figs. 3A–E), with the exception of T = 3 particles from CP-NΔ62, where a number of

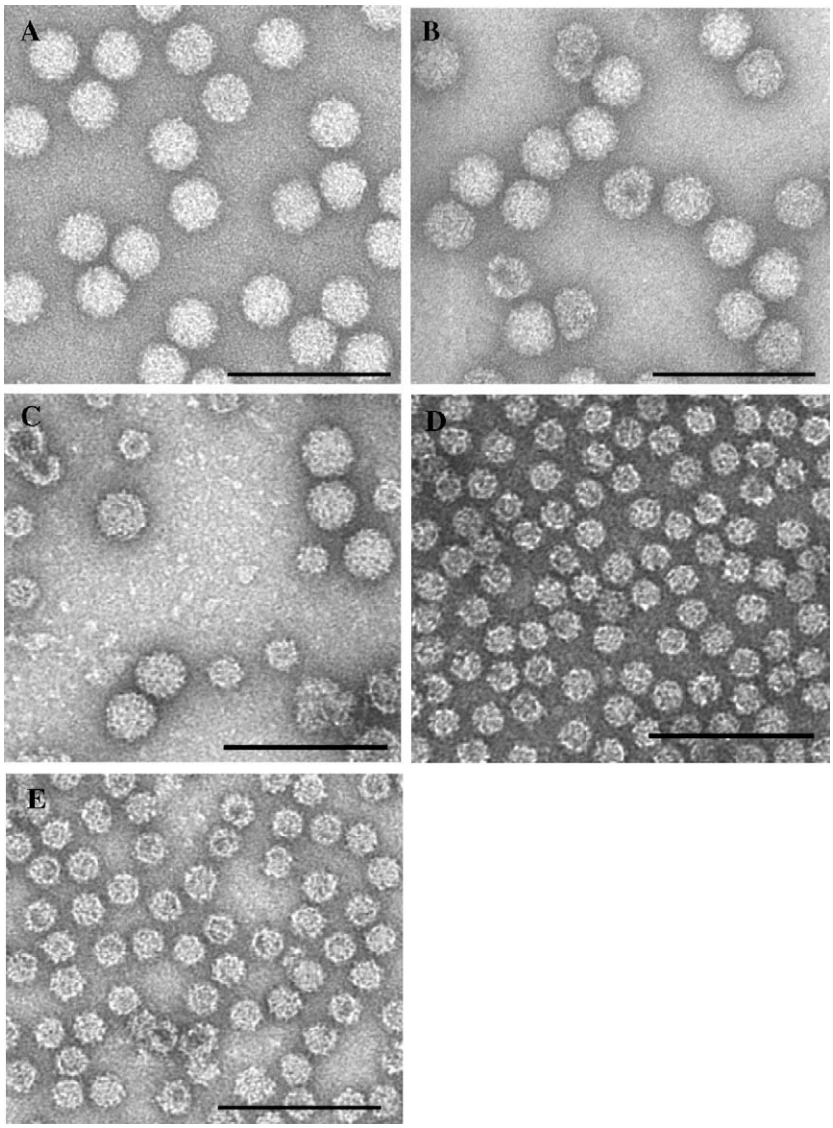

Fig. 3. Electron micrographs of TBSV particles. Micrographs showing the formation of particles of different TBSV CP-phenotypes. (A) CP-FL, (B) CP-NΔ52, (C) CP-NΔ62 (T = 3), (D) CP-NΔ62 (T = 1) and (E) CP-NΔ72. Scale bar = 100 nm.

stain-permeated broken particles are seen (Fig. 3C). The observation of full particles is not surprising, as it was suggested that viral or heterologous RNA induced the assembly of TCV capsids (Sorger et al., 1986; Stockley et al., 1986). The packaged RNAs were extracted from the respective particles and analyzed by agarose gel electrophoresis. Fig. 4 shows that the packaged nucleic acids contain a collection of RNAs ranging from 100–1900 bp. Since there is no specific band corresponding to the size of full-length mRNAs (~1100 bases), we did not further characterize the origin of the packaged RNA as it is not the scope of the current work. However, it is quite possible that the packaged RNAs contain a mixture of degraded mRNAs and cellular RNAs as was observed in similar investigations (Agrawal and Johnson, 1995; Dong et al., 1998; Lokesh et al., 2002; Schneemann and Marshall, 1998; Taylor et al., 2002). It is interesting to note that even though all or most of the N-terminal basic residues were deleted, the T = 1 particles formed by the CP-NΔ62 and CP-NΔ72 proteins appear to package RNA (Fig. 4).

The TBSV-CP of 388 amino acids (AA) is 37 residues longer than the TCV-CP of 351 AAs. Alignment of the two coat protein (CP) sequences resulted in 291AA pairs aligned with 21% sequence identity (Fig. 5). The majority of the additional (21) residues in TBSV are located in the R-domain, upstream of the β-annulus forming region of residues 67–85. Since the last basic amino acid upstream of the conserved β-annulus region of TBSV is found at the residue 65, it was assumed that the R-domain comprises residues 1–65. Therefore, a larger number (65) of amino acids are involved in forming the R-domain of TBSV compared to that of TCV (52 AAs). Interestingly, the number of basic AAs is identical (12) in the R-domains of both TBSV and TCV with the last basic AA located at positions 65 and 57, respectively, before the start of the conserved β-annulus forming region. The N-terminal deletion mutants CP-NΔ52, CP-NΔ62 and CP-NΔ72 of TBSV contain 7, 2 and 0 basic residues respectively upstream of the β-annulus region. The corresponding VLPs of CP-NΔ52 (T = 3), CP-NΔ62 (T = 3 and

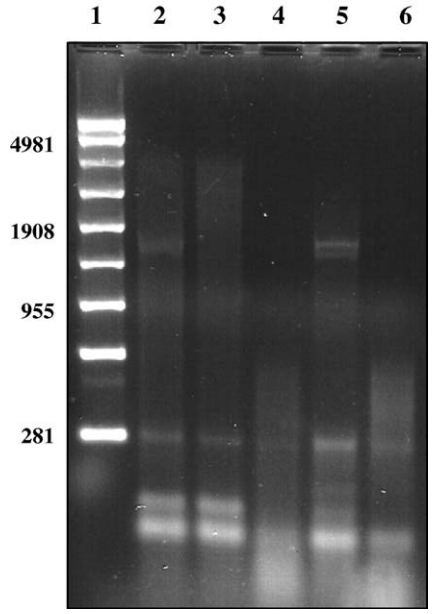

Fig. 4. Agarose gel electrophoresis of RNA. Gel electrophoretic profile of RNA extracted from different TBSV-CP phenotypes. Lanes 1: RNA marker (Promega, Madison, WI), few sizes in bases are shown on the left side, 2: CP-FL, 3: CP-NΔ52, 4: CP-NΔ62 (T = 3), 5: CP-NΔ62 (T = 1) and 6: CP-NΔ72.

T = 1) and CP-NΔ72 (T = 1) suggest that the length and possibly the number of positively charged residues in the R-domain may play a role in the formation of T = 3 capsids. The efficient formation of the T = 3 capsids by the CP-NΔ52 suggests that the last 13 residues of R-domain that include 7 of the total 12 basic residues in the R-domain are adequate for the formation of T = 3 capsids. These observations coupled with the results on CP-NΔ62, which forms both type of particles (T = 3 and T = 1), we hypothesize that as few as 3 residues of the R-domain, beyond the β-annulus forming region, maybe sufficient to form T = 3 particles of TBSV. These results clearly demonstrate that only a few residues (3–13) of the 65 residue R-domain are required for the formation of T = 3 capsids and conceivably, the same holds true for TCV capsids as well.

Similar results have been reported on Sesbania mosaic virus (SeMV), where deletion of 36 or 65 residues from the N-terminus of CP resulted in T = 1 particles, compared to the full-length CP and CP-NΔ22 yielded T = 3 particles (Lokesh et al., 2002; Sangita et al., 2004; Satheshkumar et al., 2004). Since the presence of the arm region by itself or together with a segment forming the β-annulus region was not sufficient to produce larger (T = 3) particles, Savithri and coworkers suggested the need for at least part of the R-domain, also known as the arginine rich motif for the formation of T = 3 particles (Lokesh

```
TBSV_CP MAMVKRNNNTGMIPVSTKQLLALGAAAGATALQGFVKNNGMAIVEGAVDL   50
TCV_CP  -----------MENDPRVRKFASDGAQWAIKWQ----------KKGWSTL   29
                   *   .  : :* ..*  *   *           :*   *

TBSV_CP TKRAYKAVRRRGGKKQQMINHVGGTGGAIMAPVAVTRQLVGSKPKFTGRT  100
TCV_CP  TSRQKQTARAAMGIKLSPVAQPVQKVTRLSAPVALAYREVSTQPRVSTAR   79
        *.*  ::.*   * * . : :   .   : ****:: : *.::*:.:

TBSV_CP SGSVTVTHREYLSQVNNSTGFQVNGGIVGNLLQLNPLNGTLFSWLPAIAS  150
TCV_CP  DG-ITRSGSELITTLKKNTDTEP----KYTTAVLNPSEPGTFNQLIKEAA  124
        .* :* :  * :: :::.*. :       .   *** :   *. *   *:

TBSV_CP NFDQYTFNSVVLHYVPLCSTTEVGRVAIYFDKDSEDPEPADRVELANYSV  200
TCV_CP  QYEKYRFTSLRFRYSPMSPSTTGGKVALAFDRDAAKPPPNDLASLYNIEG  174
        ::::* *.*: ::* *:..:*  *:**: **:*: .* * * ..* * .

TBSV_CP LKETAPWAEAMLRVPTDKIKRFCDDSSTSDHKLIDLGQLGIATYGGAGTN  250
TCV_CP  CVSSVPWTGFILTVPTDSTDRFVADG-ISDPKLVDFGKLIMATYGQGAND  223
          .:.**:  :* ****. .**  *.  ** **:*:*:* :**** ...:

TBSV_CP AVGDIFISYSVTLYFPQPTNTLLSTRRLDLAGALVTASGPGYLLVSRTAT  300
TCV_CP  AAQLGEVRVEYTVQLKNRTGSTSDAQIGDFAGVKD-----GPRLVSWSKT  268
        *.    :  . *: : : *.:  .::  *:**.       *  *** : *

TBSV_CP VLTMTFRATGTFVISGTYRCLTATTLGLAGGVNVNSITVVDNIGTDSAFF  350
TCV_CP  KGTAGWEHDCHFLGTGNFSLTLFYEKAPVSGLENADASDFSVLGEAAAGS  318
          *  :.    *: :*.:         . ..*::  . : .. :*  :*

TBSV_CP INCTVSNLPSVVTFTSTGITSATVHCVRATRQNDVSLI  388
TCV_CP  VQWAG----VKVAERGQGVKMVTTEEQPKGKLQALRI-  351
        :: :       *:  . *:. .*..     : : : :
```

Fig. 5. Sequence alignment. The CP sequence of TBSV (Swiss-Prot-ID: P11689) aligned with that of Turnip Crinkle Virus (TCV) (Swiss_Prot_ID: P06663). The stars indicate the locations of identical residues, while ':' and '.' correspond to functionally homologous and related residues, respectively. The entire R-domain including the Arginine rich basic amino acids of TBSV is shown in gray color.

et al., 2002; Sangita et al., 2004). Prior to that based on the proteolysis and reassembly experiments on TCV coat protein dimers, it was suggested that the R-domain and the arm may be required for the formation of T = 3 capsids (Sorger et al., 1986). However, because of the limited nature of the latter study, the extent of the R-domain and the arm regions of the CP required for the formation of T = 3 capsids was not very clear, particularly in the family of Tombusviridae. Our results reported in this study, especially on the CP-NΔ62 phenotype, suggest that even 3 residues of the R-domain containing two basic residues, upstream of the β-annulus forming region are sufficient to produce T = 3 capsids. However, efficient formation of T = 3 capsids by the CP-NΔ52 suggests that a slightly larger R-domain (13 residues) with more basic residues (7) may be necessary for the "error free assembly" of T = 3 capsids. The majority of viruses have evolved over long time periods, hence the complete R-domain may be functionally important for an efficient and selective packaging of viral genomes, delivery, replication and other aspects of the viral life cycle in plants. Our results taken together with the previous reports on SeMV (Lokesh et al., 2002; Sangita et al., 2004; Satheshkumar et al., 2004) suggest a common theme for the formation of T = 3 capsids, namely that the peptide arm, also known as βA, alone or together with β-annulus forming region, is not sufficient for the formation of T = 3 capsids.

Recent studies on the specific role of basic amino acids and β-annulus regions of SeMV or lack of it in the formation T = 3 particles point to the requirement on the length of polypeptide chain in these regions rather than the AA composition (Satheshkumar et al., 2005). They also point out that origin of the formation of β-annulus structure, which is stabilized primarily by main chain–main chain hydrogen bonds, is a consequence of capsid assembly rather than the result of specific AA sequence motif. Even though some sequences might have evolved to preferentially form such structures, they may not be absolutely essential. In other words, capsid assembly may facilitate the formation of such structures if there are sufficient number of amino acids present upstream of β-annulus forming region. This "sufficient" number of AAs might depend on a particular CP subunit forming the T = 3 capsid. However, the basic amino acids present in the R-domain are required for encapsidation of viral or cellular RNA. This hypothesis is in agreement with our results in this study as well as Savithri and Co-workers (Lokesh et al., 2002; Satheshkumar et al., 2005; Satheshkumar et al., 2004). The requirement of the R-domain in terms of its length, composition and the resulting protein–nucleic acid interactions presumably is a "means to the end" for correctly positioning the β-annulus and βA in place thereby facilitating the efficient formation of the T = 3 capsids and RNA encapsidation.

Materials and methods

Cell culture

Spodoptera frugiperda cells (line IPLB-Sf21) were grown at 27 °C in TC100 medium (Invitrogen, Carlsbad, CA) supplemented with 0.35 g of $NaHCO_3$ per liter 2.6 g of tryptose broth per liter, 2 mM L-glutamine (final concentration), 100 U of penicillin per mL and 100 μg of streptomycin per mL and 10% heat-inactivated fetal bovine serum (Schneemann et al., 1993). Cultures were maintained as monolayers in screw-capped plastic flasks or as suspensions in 1-L spinner flasks.

Generation of recombinant baculoviruses expressing TBSV coat protein

The cDNA clone of TBSV-CP in plasmid pTCTBcp (Hearne et al., 1990; Hillman et al., 1989) was a generous gift of Drs. T.J. Morris and F. Qu (University of Nebraska, Lincoln, Nebraska). In order to generate recombinant baculovirus, the full-length or mutant TBSV-CP sequence was inserted into a baculovirus transfer vector, pBacPAK9 (BD Biosciences-Clontech, Mountain View, CA). TBSV-CP full-length or truncated sequences were amplified by PCR from the pTCTBcp plasmid. To facilitate cloning of inserts into the multiple cloning site of pBacPAK9, a *Bam*HI and a *Xho*I restriction site sequences were added to the 5′ and 3′ ends of the CP sequences, respectively. The 5′ primers are BTSTART (to amplify full-length CP) 5′ GGATCCATGGCAATGGTAAAG AGAAACAACAAC3′, BT52 (to amplify CP-NΔ52) 5′CGGGATCCATGAAAA-GAGCGT ACAAAGCAGTC3′, BT62 (to amplify CP-NΔ62) 5′GGATCCATGGGAGGTAA GAACAGCAGATG3′ and BT70 (to amplify CP-NΔ72) 5′CGGGATCCATGGTA GGTGGTACAGGTGGTGC3′. The XTRev reverse primer, 5′ CTCGAGCTAAATTAG AGAAACATCATTCTGTCG3′ used in all PCR reactions, anneals to the C-terminus of the TBSV-CP and also adds a TAG stop codon to the end of all CP sequence inserts. All PCR reactions were performed using Expand High Fidelity Polymerase® (Roche, Indianapolis, IN). Amplified PCR products were first cloned into PCR2.1 TA cloning vector (Invitrogen, Carlsbad, CA) and were sequenced and aligned with the published TBSV-CP sequence (GenBank accession: M21958). Confirmed constructs digested with *Bam*HI and *Xho*I restriction enzymes were subcloned into respective sites of pBacPAK9 transfer vector. Recombinant baculoviruses expressing different TBSV-CPs were generated by co-transfecting each of the pBacPAK9 plasmid constructs with linearized baculovirus DNA in pBacPAK6, according to manufacturer's instructions (BD Biosciences Clontech). Cultures containing recombinant baculovirus were plaque purified and amplified to obtain pure stocks of each construct with high viral titers.

Protein expression and purification of VLPs

Sf-21 cells were plated at a density of 8×10^6 cells per 10 cm tissue culture dish and were infected with stocks of the respective recombinant baculoviruses at an MOI of 0.5–2 pfu per cell. Cells and supernatant were harvested 72–96 h post-infection. Nonidet P-40 was added to a final concentration of 1% (v/v) and incubated on ice for 10 min to lyse the cells. Cell debris was pelleted by centrifugation at 13,800×*g* for 10 min at 4 °C in a JA17 rotor (Beckman, Fullerton, CA). The VLPs in the

supernatant were pelleted through a 30% sucrose (wt/wt) cushion by ultracentrifugation at 184,048 × *g* for 2.5 h in a 50.2 Ti rotor (Beckman) at 4 °C. Pellets were then resuspended in the sodium acetate buffer (100 mM $C_2H_3NaO_2$, 50 mM NaCl, 10 mM $CaCl_2$ and pH 5.5) overnight at 4 °C. Insoluble material in the resuspended pellet was removed by centrifugation at 12, 000 × *g* for 10 min in a micro-centrifuge. The supernatant was analyzed by SDS-PAGE analysis using 10–20% Tris-Glycine gel and stained with Simply Blue stain (Invitrogen, Carlsbad, CA) as well as dot blot analysis. To further purify VLPs, the supernatant was loaded onto 10–40% sucrose gradients (wt/wt) made in sodium acetate buffer and centrifuged at 197, 500 × *g* for 2 h in a SW-41 rotor (Beckman). VLPs were harvested from gradients by puncturing the sides of the tubes with a needle and aspirating the bands using a syringe or by ISCO gradient fractionator (Teledyne, Los Angeles, CA) at 0.75 mL/min and 0.5 min per fraction.

Immunodetection of TBSV coat protein

Both cell lysates collected from Sf-21 cells infected with recombinant baculovirus and purified VLPs were assayed by Western dot blot for detecting the expression of TBSV protein. Samples were applied as dots onto a nitrocellulose membrane and allowed to air dry for 5 min at room temperature. A positive control consisted of native TBSV particle antigens, a gift of Dr. H.B. Scholthof (Texas A and M University, College Station, Texas). The membrane was then incubated at room temperature (RT) for 1 h in a blocking buffer made of 1% non-fat dry milk in phosphate-buffered saline (PBS). After blocking, the membrane was treated for 1 h at RT with rabbit anti-TBSV antibody (ATCC, Manassas, VA) diluted-1000 fold in the blocking buffer containing 0.05% Tween 20. The membrane was then washed twice for 15 min at RT with washing buffer made of 0.05% Tween in PBS. Afterwards, the membrane was incubated for 30 min at RT in blocking buffer containing a 2000-fold dilution of anti-rabbit IgG conjugated to horseradish peroxidase (Amersham, Piscataway, NJ). Following incubation, the membrane was washed four times in washing buffer. Antigen–antibody complexes were visualized by incubation of blot in Super Signal West Pico Chemiluminescent substrate (Pierce Biotechnology, Rockford, IL).

Pooled sera from three mice, hyper-immunized with purified TBSV-CP(NΔ52) VLPs were examined in a enzyme linked immunosorbent assay (ELISA). Approximately 1 μg/well of TBSV-VLP antigens either native or denatured by heating (10 min at 90 °C) in mixture of SDS and β-mercaptoethanol was coated on ELISA plates (Immunolon II, Dynatech Laboratories Inc., Chantilly, VA) in a coating buffer (15 mM sodium carbonate, 35 mM sodium bicarbonate buffer, pH 9.6) overnight. The wells were blocked by 1% bovine serum albumin in a tris-buffered saline (TBS, 50 mM Tris–HCl, 140 mM saline, pH 8.0) for 1 h at RT. Each well was exposed to serial dilutions of hyper-immune serum for 1 h at RT. After the wells were treated with wash buffer (TBST,0.25% tween-20 in TBS) three times, they were exposed to horse radish peroxidase-labeled anti-mouse antibody (Pierce Biotechnology, Rockford, IL) diluted (1:10,000) in wash buffer for 1 h at RT. The wells were washed three times with wash buffer and the bound antibodies were detected with a TMB-peroxidase kit (Kirkegaard and Perrry Laboratories Inc., Gaithesburg, MD). Substrate reaction was stopped with 1N hydrochloric acid and the absorbance at 450 nm was determined using a Versamax® microplate reader (Molecular Devices, Sunnyvale, CA).

Extraction of RNA from VLPs and agarose gel electrophoresis

RNA was extracted from purified VLPs with acidic phenol-chloroform after the addition of sodium chloride and SDS to a final concentration of 0.2 M and 0.1%, respectively. RNA in the aqueous fraction was precipitated with 0.3 M sodium acetate (pH 5.2) and 1 μg of glycogen as a carrier. RNA pellet was washed in 70% ethanol, vacuum dried and resuspended in nuclease-free water. Approximately 2 μg of RNA was loaded on 1% agarose gel made in MOPs buffer (0.02 M MOPS, pH 7.0, 2 mM sodium acetate, 1 mM EDTA, pH8.0) with formaldehyde to eliminate secondary structures. The RNA gels were subjected to gel electrophoresis in MOPs buffer with formaldehyde at 150 V for 1.5 h. RNA bands were visualized by staining with ethidium bromide.

Electron microscopy

Carbon-coated, copper grids were glow discharged in the presence of amyl acetate immediately before loading samples. Grids were placed in 10 μL of VLP samples for 1 min, washed three times in sterile filtered water and stained in 10 μL drops of 1% uranyl acetate three times allowing the grids to soak in the last drop of stain for 2 min. After drying grids, samples were examined under an electron microscope (Phillips CM100).

Acknowledgments

The authors are extremely grateful for the cDNA clones of TBSV provided to them by Drs. Jack Morris and Feng Qu of University of Nebraska, Lincoln, Nebraska. The authors thank Dr. H.B. Scholthof (Texas A and M University, College Station, TX) for the gift of native TBSV particles. Authors would also like to acknowledge Dr. Mark Olson of USAMRIID, Fort Detrick, MD, for stimulating discussions. We thank Dr. Craig Shepherd for critically reading the manuscript. The work reported in this manuscript was fully supported by a contract, W81XWH-04-2-0027, from U.S. Army to V.S.R.

References

Agrawal, D.K., Johnson, J.E., 1995. Assembly of the T = 4 Nudaurelia capensis omega virus capsid protein, post-translational cleavage, and specific encapsidation of its mRNA in a baculovirus expression system. Virology 207 (1), 89–97.

Crowther, R.A., Amos, L., 1971. Three dimensional reconstruction of some spherical viruses. Cold Spring Harbor Symp. Quant. Biol. 36, 489–494.

DeLano, W.L., 2002. The PyMol Molecular Graphics system. World Wide Web http://www.pymol.org.

Dong, X.F., Natarajan, P., Tihova, M., Johnson, J.E., Schneemann, A., 1998. Particle polymorphism caused by deletion of a peptide molecular switch in a quasiequivalent icosahedral virus. J. Virol. 72 (7), 6024–6033.

Harrison, S.C., 1971. Structure of Tomatio Bushy Stunt Virus: three-dimensional X-ray diffraction analysis at 30A resolution. Cold Spring Harbor Symp. Quant. Biol. 36, 495–501.

Harrison, S.C., Olson, A.J., Schutt, C.E., Winkler, F.K., 1978. Tomato bushy stunt virus at 2.9 Å resolution. Nature 276, 368–373.

Hearne, P.Q., Knorr, D.A., Hillman, B.I., Morris, T.J., 1990. The complete genome structure and synthesis of infectious RNA from clones of tomato bushy stunt virus. Virology 177 (1), 141–151.

Hillman, B.I., Hearne, P., Rochon, D., Morris, T.J., 1989. Organization of tomato bushy stunt virus genome: characterization of the coat protein gene and the 3′ terminus. Virology 169 (1), 42–50.

Hogle, J.M., Maeda, A., Harrison, S.C., 1986. Structure and assembly of turnip crinkle virus: I. X-ray crystallographic structure analysis at 3.2 A resolution. J. Mol. Biol. 191 (4), 625–638.

Joelson, T., Akerblom, L., Oxelfelt, P., Strandberg, B., Tomenius, K., Morris, T.J., 1997. Presentation of a foreign peptide on the surface of tomato bushy stunt virus. J. Gen. Virol. 78 (Pt. 6), 1213–1217.

Li, T.C., Takeda, N., Kato, K., Nilsson, J., Xing, L., Haag, L., Cheng, R.H., Miyamura, T., 2003. Characterization of self-assembled virus-like particles of human polyomavirus BK generated by recombinant baculoviruses. Virology 311 (1), 115–124.

Lokesh, G.L., Gowri, T.D., Satheshkumar, P.S., Murthy, M.R., Savithri, H.S., 2002. A molecular switch in the capsid protein controls the particle polymorphism in an icosahedral virus. Virology 292 (2), 211–223.

Olson, A.J., Bricogne, G., Harrison, S.C., 1983. Structure of tomato busy stunt virus IV. The virus particle at 2.9 A resolution. J. Mol. Biol. 171 (1), 61–93.

Pettersen, E.F., Goddard, T.D., Huang, C.C., Couch, G.S., Greenblatt, D.M., Meng, E.C., Ferrin, T.E., 2004. UCSF Chimera—A visualization system for exploratory research and analysis. J. Comput. Chem. 25 (13), 1605–1612.

Sangita, V., Lokesh, G.L., Satheshkumar, P.S., Vijay, C.S., Saravanan, V., Savithri, H.S., Murthy, M.R., 2004. T = 1 capsid structures of Sesbania mosaic virus coat protein mutants: determinants of T = 3 and T = 1 capsid assembly. J. Mol. Biol. 342 (3), 987–999.

Satheshkumar, P.S., Lokesh, G.L., Sangita, V., Saravanan, V., Vijay, C.S., Murthy, M.R., Savithri, H.S., 2004. Role of metal ion-mediated interactions in the assembly and stability of Sesbania mosaic virus T = 3 and T = 1 capsids. J. Mol. Biol. 342 (3), 1001–1014.

Satheshkumar, P.S., Lokesh, G.L., Murthy, M.R., Savithri, H.S., 2005. The role of arginine-rich motif and beta-annulus in the assembly and stability of Sesbania mosaic virus capsids. J. Mol. Biol. 353 (2), 447–458.

Schneemann, A., Marshall, D., 1998. Specific encapsidation of nodavirus RNAs is mediated through the C terminus of capsid precursor protein alpha. J. Virol. 72 (11), 8738–8746.

Schneemann, A., Dasgupta, R., Johnson, J.E., Rueckert, R.R., 1993. Use of recombinant baculoviruses in synthesis of morphologically distinct virus like particles of flock house virus, a nodavirus. J. Virol. 67 (5), 2756–2763.

Scholthof, H.B., Morris, T.J., Jackson, A.O., 1993. The Capsid protein gene of tomato bushy stint virus is dispensable for systemic movement and can be replaced for localized expression of foreign genes. Mol. Plant-Microbe Interact. 6, 309–322.

Shepherd, C.M., Borelli, I.A., Lander, G., Natarajan, P., Siddavanahalli, V., Bajaj, C., Johnson, J.E., Brooks III, C.L., Reddy, V.S., 2006. VIPERdb: a relational database for structural virology. Nucleic Acids Res. 34, D386–D389 (Database issue).

Sorger, P.K., Stockley, P.G., Harrison, S.C., 1986. Structure and assembly of turnip crinkle virus: II. Mechanism of reassembly in vitro. J. Mol. Biol. 191 (4), 639–658.

Stockley, P.G., Kirsh, A.L., Chow, E.P., Smart, J.E., Harrison, S.C., 1986. Structure of turnip crinkle virus: III. Identification of a unique coat protein dimer. J. Mol. Biol. 191 (4), 721–725.

Taylor, D.J., Krishna, N.K., Canady, M.A., Schneemann, A., Johnson, J.E., 2002. Large-scale, pH-dependent, quaternary structure changes in an RNA virus capsid are reversible in the absence of subunit autoproteolysis. J. Virol. 76 (19), 9972–9980.

JOURNAL OF VIROLOGY, Feb. 2007, p. 1119–1128 Vol. 81, No. 3
0022-538X/07/$08.00+0 doi:10.1128/JVI.01909-06

Presence of a Surface-Exposed Loop Facilitates Trypsinization of Particles of Sinsiro Virus, a Genogroup II.3 Norovirus▽

Shantanu Kumar,[1] Wendy Ochoa,[1] Shinichi Kobayashi,[2] and Vijay S. Reddy[1]*

Department of Molecular Biology, The Scripps Research Institute, 10550 North Torrey Pines Road, La Jolla, San Diego, California 92037,[1] and Laboratory of Virology, Aichi Prefectural Institute of Public Health, Nagoya, Aichi 462-8576, Japan[2]

Received 1 September 2006/Accepted 25 October 2006

Noroviruses (NoVs) are the causative agents of nonbacterial acute gastroenteritis in humans. NoVs that belong to genogroup II (GII) are quite prevalent and prone to undergo recombination, and their three-dimensional structure is not yet known. Protein homology modeling of Sinsiro virus (SV), a member of the GII.3 NoVs, revealed the presence of a surface-exposed 20-amino-acid (aa) insertion in the P2 domain of the capsid protein (CP) relative to the Norwalk virus (NV) CP, which is a well known hot spot for mutations to counter the host immunological response. To further characterize the role of the long insertion in SV, the capsid protein gene was expressed using the recombinant baculovirus system. Trypsinization of the resultant virus-like particles yielded two predominant bands (31.7 and 26.1 kDa) in sodium dodecyl sulfate-polyacrylamide gel electrophoresis and Western blot analysis. N-terminal sequencing and analysis of the mass spectroscopic data indicated that these fragments correspond to residues 1 to 292 (26.1 kDa) and 307 to 544 (31.7 kDa). In addition, the above data taken together with the comparative modeling studies indicated that the trypsin cleavage sites of the Sinsiro virus CP, Arg292 and Arg307, are located at the beginning of and within the 20-aa insertion in the P2 domain, respectively. This study demonstrates that the presence of the surface-exposed loop in the GII.3 NoVs facilitates the trypsinization of the capsid protein in the assembled form. The SV particles remain intact even after trypsin digestion and retain the suggested receptor binding linear epitope of residues 325 to 334. The above results are distinct from those obtained from the trypsinization studies performed earlier on the NV (GI) and VA387 (GII) viruses, both of which lack the large surface insertion and associated basic residues. These new observations may have implications for host receptor binding, cell entry, and norovirus infection in general.

Human noroviruses (NoVs) are causative agents of nonbacterial acute gastroenteritis, second only to rotaviruses, in all age groups of humans and are associated with significant morbidity worldwide and substantial mortality in developing countries (12, 15, 21, 25). They belong to the genus *Norovirus* in the family *Caliciviridae*. The rates of infection with NoVs are high, and the viruses spread rapidly from person to person primarily via the fecal-oral route, resulting in large outbreaks of disease that often persist. The magnitude of genetic and antigenic diversity among NoV strains came to light in the past several years due to greater surveillance of disease outbreaks and rapid availability and analysis of sequence data (1, 12, 13, 24, 38, 41). The NoV strains that infect humans are classified into two major genogroups, genogroup I (GI) and GII. The GII strains exhibit greater virulence, as they are prone to undergo recombination, and they cause the majority of gasteroenteritis worldwide (14, 19, 22, 30, 31, 42).

NoVs are spherical with a diameter of ~35 nm and contain a single-stranded, positive-sense, polyadenylated RNA genome of 7,400 to 7,700 nucleotides (2). The genome is divided into three open reading frames (ORFs). ORF1 encodes a 200-kDa polyprotein, which is further processed into at least six nonstructural proteins. ORF2 codes for the ~60-kDa capsid protein (CP) VP1, and ORF3 encodes a minor structural protein, VP2, which is basic in nature (15, 28). Studies on the life cycle and pathogenesis of NoVs have been hampered by the lack of an appropriate cell culture system. However, the ability to generate virus-like particles (VLPs) from insect cells infected with recombinant baculoviruses expressing the coat protein (VP1) and in vitro studies of binding to histo-blood group antigens has led to significant advances related to NoV structure, function, and biophysical properties (3, 7, 20, 29).

The three-dimensional (3D) structures of Norwalk virus (NV) VLPs and San Miguel sea lion virus, a member of the genus *Vesivirus* (GII.2) in the family *Caliciviridae*, have been determined at near-atomic resolution (10, 29). Typically, NV capsids are composed of 180 copies of a coat protein (VP1) assembled into T = 3 icosahedral virions. However, it has been reported that sometimes VP1 subunits form smaller capsids, which consists of 60 subunits with T = 1 icosahedral symmetry (40). The tertiary structure of the NV capsid protein contains two major structural domains: the shell (S) domain with a canonical β-barrel fold and the protruding (P) domain. The S domain consists of the N-terminal 225 amino acids (aa), and the P domain is composed of 226 to 530 aa. The P domain is further divided into two subdomains, P1 and P2. The P1 domain comprises aa 226 to 278 and 406 to 530. The P2 domain is a 127-aa insertion (aa 279 to 405) in the P1 domain; it is the most distal part of the folded coat protein (VP1) and is located at the exterior surface of the capsid (29). The P2 domain is therefore predicted to contain the antigenic determinants of the immunological response of the host. A binding surface that

* Corresponding author. Mailing address: Department of Molecular Biology, TPC-6, The Scripps Research Institute, 10550 North Torrey Pines Road, La Jolla, CA 92037. Phone: (858) 784-8191. Fax: (858) 784-8688. E-mail: reddyv@scripps.edu.

▽ Published ahead of print on 1 November 2006.

interacts with the human histo-blood group antigens was mapped onto the P2 domain by computational analysis and later confirmed by site-directed mutagenesis (35). Recently, Lochridge et al. identified amino acids 291 to 293 and 313 to 322 as the likely antigenic epitopes in the P2 domains of NV and Snow Mountain virus, which are the reference strains of GI.1 and GII.2, respectively (23). The linear epitope composed of amino acids 313 to 322 in Snow Mountain virus, which has been suggested to be responsible for the host cell interactions, is conserved among all the NoVs (23).

Sequence analysis of the NoV capsid protein indicated that the S-domain sequences are about 30% identical, while the sequence identity drops to 11% and 8% in the P1 and P2 domains, respectively (9). Even though there are many trypsin and chymotrypsin cleavage sites across the entire capsid protein, results obtained from the proteolytic analysis of the Norwalk virus VLPs clearly indicated that the intact NV particles are resistant to trypsin digestion (18). However, trypsin digestion of the soluble protein of NV resulted in partial digestion of the capsid protein, in which the S domain was completely digested while the P domain remained intact (18). These data indicated that the P-domain structure is resistant to proteases. However, recent studies by Tan et al. contradict the above results. In particular, they suggest that the intact particles of NV and VA387, a GII.4 virus, undergo partial trypsinization near the hinge region between the S and P domains, thereby releasing the nearly intact P domain of 32 to 34 kDa (36).

Sinsiro virus (SV), the subject of the present study, belongs to the GII.3 NoVs. The capsid protein of SV is made of 548 aa residues and exhibits 98% amino acid sequence identity with other members of GII.3 NoVs (e.g., Arg320, Oberhausewn, and Toronto viruses, etc.). The prevalence of acute gastroenteritis caused by these strains suggested that they have better adaptability to circumvent the human immune response (27). The molecular and structural characterization of SV VLPs may provide further insights into their pathogenesis. Here we report the results of studies on expression of the SV capsid protein in insect cells by using a recombinant baculovirus system, three-dimensional electron microscopy (EM) reconstruction using negatively stained particles, and homology modeling of the SV capsid. In addition, we characterized the unique trypsin cleavage pattern of SV by using N-terminal sequencing, mass spectrometry analysis, and molecular modeling studies. The sequence in and around the insertion is conserved among all GII.3 and GII.6 NoVs, suggesting that these viruses undergo similar patterns of trypsinization. The results from this study may provide some of the possible reasons for the greater efficacy of virus-cell interactions involving GII.3 and GII.6 NoVs.

MATERIALS AND METHODS

Homology modeling of the SV capsid. The comparative modeling program MODELLER (version 6.0) and the default modeling options (32) were used to generate homology models of Sinsiro virus. The Norwalk virus capsid structure (PDB no. 1IHM) was used as the template due to its having greater sequence identity (47%) than the San Miguel sea lion virus (PDB no. 2GH8), which has only 17% amino acid sequence identity with SV. The amino acid sequence identity of 47% between Sinsiro and Norwalk viruses is well above the threshold (35%) for obtaining a reliable homology model. A multiple-sequence alignment was obtained by aligning the amino acid sequences of 12 different NoVs, including Sinsiro virus, to the Norwalk virus sequence, using the Clustal-w server available at http://clustalw.genome.jp/. In addition, six neighboring subunits that immediately surround the three reference subunits (A, B, and C) (http://viperdb.scripps.edu/info_page.php?VDB = 1ihm) (34) were included to impose restraints on the subunit interfaces. At the end of the modeling run, the reference subunits (A, B, and C) were extracted and used for the subsequent analysis.

Cell culture. *Spodoptera frugiperda* cells (line IPLB-Sf21) were grown at 27°C in TC100 medium (Invitrogen, Carlsbad, CA) supplemented with 0.35 g of $NaHCO_3$ per liter, 2.6 g of tryptose broth per liter, 2 mM L-glutamine (final concentration), 100 U of penicillin per ml, 100 μg of streptomycin per ml, and 10% heat-inactivated fetal bovine serum (33). Cultures were maintained as monolayers in screw-cap plastic flasks or as suspensions in 1-liter spinner flasks. Hi5 cells were grown at 27°C in ESF 921 medium (Expression System, CA) supplemented with 100 μg of penicillin per ml and 100 μg of streptomycin per ml. Cultures were maintained in suspension on a shaker (100 rpm) in a 500-ml polypropylene bottle.

Generation of recombinant baculoviruses expressing SV coat protein. The cDNA clone of Sinsiro virus capsid protein was generously provided to us by Shinichi Kobayashi (Aichi Prefectural Institute of Public Health, Nagoya, Japan) and used as a template in a PCR to amplify the full-length capsid gene (GenBank accession no. AB195226), using forward (5′CGGGATCCATGAAGATGGCG TCGAATG3′) and reverse (5′GCTCTAGATTATTGAATCCTTCTACGCCC A3′) primers having 5′ BamHI and XbaI restriction sites, respectively. PCR was performed using high-fidelity *Pfx* polymerase (Invitrogen) according to the manufacturer's instructions. Recombinant baculovirus transfer plasmids (pBPSV) containing the full-length Sinsiro virus CP sequence were generated by inserting PCR-amplified fragments flanked by BamHI and XbaI restriction enzyme sites into the multiple cloning sites of pBacPAK9 (BD Biosciences-Clontech, CA). pBSV plasmids were sequenced using Bac1 (5′ACCATCTCGCAAATAAATA 3′) and Bac2 (5′CAACGCACAGAATCTAGCG 3′) primers to confirm the accuracy of the SV sequence. Recombinant baculoviruses expressing SV CPs were generated by cotransfecting pBPSV plasmids with linearized baculovirus DNA (pBacPAK6) according to the manufacturer's instructions (BD Biosciences-Clontech). Recombinant baculoviruses were plaque purified and amplified to obtain pure stocks of viruses.

Expression and purification of rSV particles. Recombinant SV (rSV) particles were prepared and purified essentially as previously described (17). Briefly, *Trichoplusia ni* (Tn5) insect cells (2.0×10^6 cells per ml) were infected with a baculovirus recombinant expressing the capsid protein of SV at a multiplicity of infection of 5 and incubated for 3 days at 27°C in a incubator shaker maintained at 100 rpm. Nonidet P-40 was added to a final concentration of 0.5% (vol/vol) and incubated on ice for 10 min to lyse the cells. rSV particles released into the medium were separated from the cell lysate by centrifuging the culture for 15 min at 10,000 rpm in a JA-17 rotor, using a Beckman J2-21 centrifuge. The expressed protein in supernatant was concentrated by precipitation with polyethylene glycol (8%) and was further purified by centrifugation through a 30% (wt/wt) sucrose cushion for 2 h in an Ti 50.2 rotor (Beckman) at 35,000 rpm. Pellets were suspended in 0.1 M phosphate buffer (pH 6.0), layered onto 10 to 40% sucrose gradients, and centrifuged for 3 h at 26,000 rpm in an SW28 rotor. Peak fractions then were pooled, dialyzed, and stored at 4°C. Integrity of the rSV VLPs was confirmed by EM observation of particles negatively stained with 1% uranyl acetate. The protein concentrations were determined with a Bradford assay kit for quick protein estimation (Bio-Rad).

Native gel analysis. The purified VLPs were subjected to native gel analysis in 0.5% (wt/vol) agarose gels with 0.1 M Tris-malate buffer (pH 6.5) containing 0.001% (wt/vol) ethidium bromide. The electrophoresis was carried out at a constant voltage (40 V) for 3 h, and RNA was visualized in a Bio-Rad Gel Doc system. The gel was dried and stained for protein with 0.05% (wt/vol) Coomassie brilliant blue R250.

Isolation of RNA from purified particles and reverse transcription-PCR analysis. Sodium dodecyl sulfate (SDS) and NaCl were added to gradient-purified SV particles at final concentrations of 1% (wt/vol) and 0.2 M, respectively. RNA was extracted with an equal volume of acidic phenol-chloroform and precipitated with 3 volumes of ethanol in the presence of 0.3 M sodium acetate and 20 mg of glycogen. After several hours at −20°C, the RNA was pelleted, washed with 70% ethanol, dried, and dissolved in nuclease-free water, and first-strand cDNA synthesis was carried out using CP-specific antisense primers with reverse transcriptase (Invitrogen, CA). The PCR was performed using *Pfx* polymerase (Invitrogen, CA).

Production of hyperimmune antiserum in laboratory mice and ELISA. To produce hyperimmune serum, mice were immunized with rSV capsid protein. The immunization regimen consisted of one intramuscular injection of the purified rSV in Freund's adjuvant (at a dose of 60 μg per mouse) followed by two

booster injections of the same dose in Freund's incomplete adjuvant. The animals were bled 2 weeks after the last booster injection. An enzyme-linked immunosorbent assay (ELISA) was performed to quantify the titer of antibody. Briefly, the VLPs were directly applied to microplates (nun-Immuno plates) at 100 μl per well and a final concentration of 1 μg/ml in carbonate-bicarbonate buffer (0.05 M, pH 9.6) and were incubated overnight at 4°C. The antigen-coated plates were blocked for 2 h at room temperature with 5% nonfat milk in 0.01 M phosphate-buffered saline (PBS) (pH 7.2) and washed thrice with PBS containing 0.05% Tween 20 (PBST). Different dilutions of primary antisera (1:10, 1:100, 1:1,000, and 1:10,000) were incubated with the antigen for 1 h at room temperature and washed thrice with PBST. Anti-mouse immunoglobulin (Sigma) was diluted 1:10,000, and the plates were incubated for 1 h at room temperature. Following incubation, the plates were washed thrice with PBST, 3,3′,5,5′-tetramethyl benzidine (TMB)–peroxidase substrate (Sigma) was added, and the color was allowed to develop for 10 min at room temperature. The reaction was stopped by adding 1% SDS, and the optical density at 405 nm was determined with a Spectra Max-250 (Molecular Devices, CA).

Trypsin digestion of assembled and solubilized rSV protein. TPCK (*N*-tosyl-L-phenylalanine chloromethyl ketone)-trypsin was purchased from Sigma-Aldrich. Stock solutions were prepared at concentrations of 2 mg/ml in 0.001 N HCl, and serial dilutions were made in PBS (pH 7.4). Digestions of rNV particles were performed for 30 min at 37°C in reaction volumes of 20 microliters. Following incubation, reaction products were electrophoresed on 4 to 12% bis-Tris gels (Invitrogen, CA), and bands were visualized by staining with Simple blue as described by the manufacturer (Invitrogen, CA). Disassociation of VLPs was performed by dialyzing rSV particles overnight at 4°C in 50 mM Tris (pH 8.9). Samples were also visualized under EM to confirm the disassembly of VLPs. Digestion of solubilized rSV protein was performed as described for the assembled particles.

Gradient purification of trypsin-digested rSV particles was done by treating the VLPs (1 mg/ml) with trypsin (62.5 μg/ml) at 37°C for 30 min in a reaction volume of 1.0 ml. This was followed by layering 500 μl of the digested VLPs on a continuous 10 to 40% sucrose gradient and centrifuging for 2 h in an SW41 rotor (Beckman), and fractions were collected by bottom puncture and analyzed by SDS-polyacrylamide gel electrophoresis (SDS-PAGE) and Western blot analysis.

SDS-PAGE and immunoblotting analysis. Samples to be analyzed were boiled for 2 min in sample buffer containing 2% SDS, 100 mM dithiothreitol, 0.05 M Tris-HCl (pH 6.8), 10% glycerol, and 0.1% bromophenol blue. Proteins were analyzed on 4 to 12% bis-Tris gels according to the manufacturer's instructions (Invitrogen, CA). The proteins separated by SDS-PAGE were transferred onto a polyvinylidene difluoride (PVDF) membrane (Invitrogen, CA) as described by manufacturer. The full-length SV and trypsin-digested SV capsid protein were detected using a mouse hyperimmune anti-rSV serum at a dilution of 1:5,000 in PBS. The secondary antibodies used were conjugated to horseradish peroxidase (Chemicon International, CA). The membrane was developed with SuperSigna West Pico chemiluminescent substrate (Pierce Biotechnology, Inc., IL) according to the manufacturer's protocol.

Transmission EM (TEM). Negative-stain EM was used to analyze the presence, integrity, and morphology of the rSV VLPs. Uranyl acetate (1%; pH 5.0) was used to stain the samples. A drop of the sample (10 μl) was placed on glow-discharged, carbon-coated, 400-mesh copper grids (Ted Pella Inc., Redding, CA) for 1 min at room temperature. The grids were washed three times by being transferred into drops of water placed on Parafilm, and the excess liquid was blotted off from the side of the grid with a filter paper. The grids were then stained by quickly immersing them (twice) into drops of uranyl acetate solution and finally were placed in a third drop of uranyl acetate stain for 1 min, and excess liquid was blotted out as before. The grids were then air dried for 5 min at room temperature and examined under a CM100 microscope (Phillips) at 80 kV at a magnification of ×45,000, and photographs were recorded at a magnification of ×52,000.

Reconstruction of negatively stained VLPs. The VLP samples at a concentration of 4 mg/ml were placed on glow-discharged carbon film and stained briefly with 2% uranyl acetate. The grids were observed in a Philips Tecnai F20 transmission electron microscope operated at 120 kV. Digital images were recorded using low-irradiation procedures (~20 electrons/Å^2), and those that displayed minimal astigmatism and drift as assessed by visual inspection and diffraction were selected for further analysis. Particles separated from their neighbors and with a clear background were selected and masked as individual images by using the software ROBEM (6). The image intensity values were adjusted to remove linear background gradients and to normalize the means and variances of the data (8). The initial orientation and origin parameters of the images for the reconstruction were determined by a model-based refinement approach. An electron density map was calculated from the X-ray coordinates of Norwalk virus (PDB no. 1IHM) and used as an initial model. The translation (x, y) and orientation (0, 0, w) parameters were refined for each particle by use of repeated cycles of correlation procedures (4–6). Images were typically discarded if they showed a correlation coefficient, calculated between the raw image and the corresponding projected view of an intermediate reconstruction, of less than one standard deviation of the mean correlation coefficient of the entire data set. A complete refinement protocol was carried out using the EM3DR package (6). The final maps were computed using a total of 184 individual particles.

Mass spectrometry and N-terminal amino acid protein sequence analysis. The molecular weights of protein were determined by matrix-assisted laser desorption ionization–time-of-flight (MALDI-TOF) mass spectrometry performed at the core facility of the Scripps Research Institute, CA. For N-terminal amino acid sequence analysis, proteins separated by SDS-PAGE were transferred onto a PVDF membrane and stained with Ponceau red, and the bands corresponding to the trypsin cleavage products, detected by Western blot analysis, were excised. N-terminal microsequencing was performed on an Applied Biosystems (ABI Procise) protein sequencer in the Protein Sequencing Core Facility at the Scripps Research Institute.

RESULTS

Production of recombinant SV VLPs by using the baculovirus expression system. A PCR-amplified 1.7-kb fragment (ORF2 of SV) was subcloned into a baculovirus transfer vector to produce a construct called pBPSV. Sequencing of pBPSV confirmed the presence and accuracy of the SV sequence. Recombinant baculoviruses expressing the coat protein of SV were isolated by transfecting the Sf21 cells with pBPSV and linearized genomic DNA, followed by plaque purification. Electrophoretic analysis of the overexpressed proteins from the infected cells showed a major band with an apparent molecular mass of 60 kDa (data not shown). Recombinant Sinsiro virus VLPs were further purified by banding on a 10% to 40% sucrose gradient, and the peak fractions were collected. SDS-PAGE analysis of the fractions highlighted the presence of a single major band of ~60 kDa (Fig. 1A). Examination of the major peak fraction (Fig. 1A, lane 6) under a transmission electron microscope by employing negative-staining procedures confirmed the presence of intact particles (Fig. 1B). These particles resembled the typical NoV particles produced in earlier studies (20). We observed mostly empty particles, as seen in the case of NV VLPs, and a few full particles having an average diameter of ~35.0 nm. However, the relative proportions of the full and empty particles varied from one preparation to another and also depended on the type of insect cells (e.g., Sf21 or Tn5) used for the baculovirus expression. Although the formation of full capsids is not a very common observation, such a finding has been reported earlier in the case of Hawaii human calicivirus (GII) (16). The gradient-purified rSV particles were used for immunizing mice. The serum samples collected from the mice showed high titers of antibodies against rSV as evaluated by ELISA (data not shown).

EM reconstruction of negatively stained rSV capsids. Since our efforts to obtain good frozen cryosamples had not been very successful so far, a preliminary 3D reconstruction of VLPs was carried out using 186 negatively stained particles, which adequately sampled the icosahedral asymmetric unit to a resolution of 26 Å. The reconstruction clearly showed that the subunits are organized in a T = 3 icosahedral arrangement with a thin contiguous shell and distinctive protrusions on the

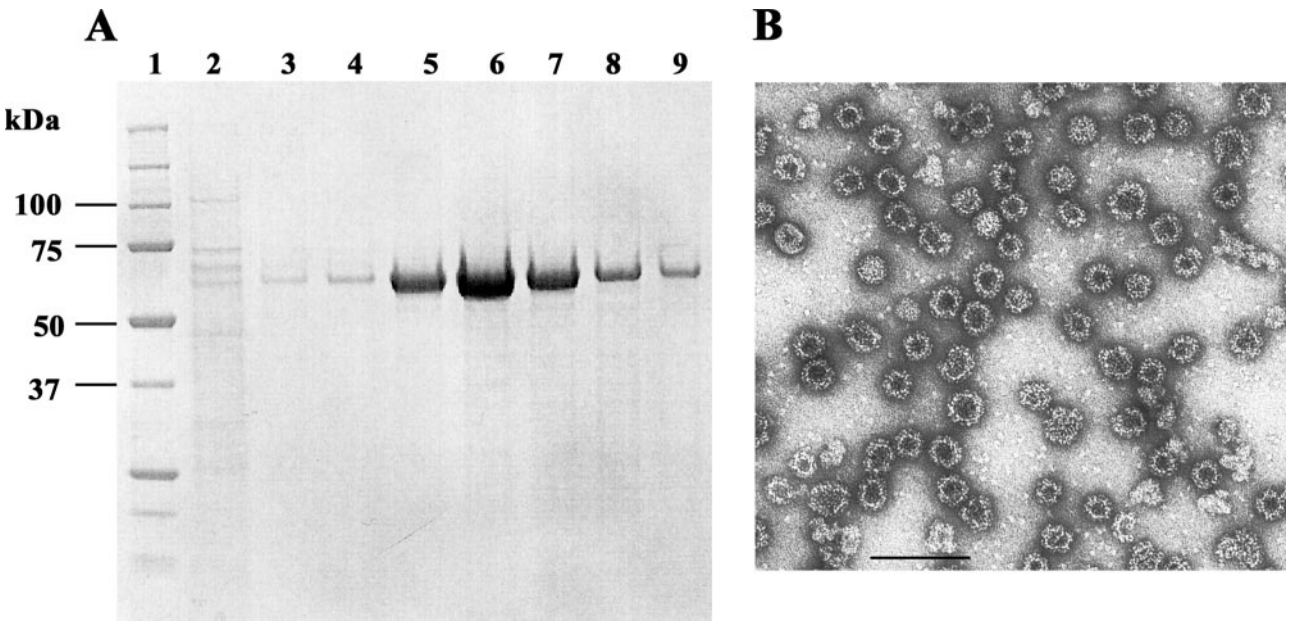

FIG. 1. SDS-PAGE analysis and electron micrographs of rSV VLPs. (A) SDS-PAGE analysis of the peak fractions of a sucrose gradient. Lane 1, molecular mass marker; lanes 2 to 9, fractions collected from the gradient. The arrow indicates a single major band of ~60 kDa. (B) Negative-stain electron microscopy of purified rSV VLPs, showing empty VLPs. Bar, 100 nm.

surface (Fig. 2A and B). A comparative analysis of this reconstruction with the 3D structure of the recombinant Norwalk virus (PDB-ID no. 1IHM) (29) showed no discernible differences at this resolution. The relative dispositions of the shell and the protruding domains appeared identical to those of Norwalk virus.

Characterization of RNA associated with VLPs. Purified rSV VLPs were analyzed on a native 0.5% agarose gel and stained with ethidium bromide to visualize the presence of RNA. The same gel was dried and stained for protein with Coomassie brilliant blue R-250. Interestingly, the VLPs stained positive for both RNA and protein (Fig. 3A and B).

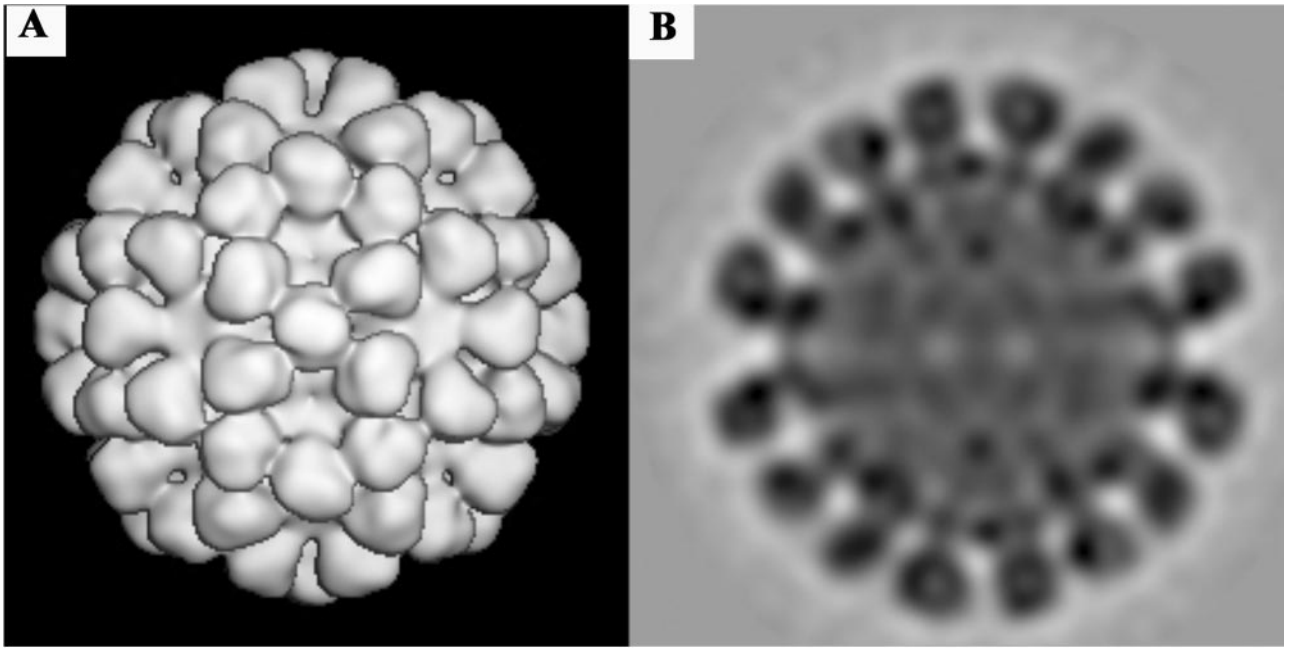

FIG. 2. Surface-shaded EM 3D density map of VLPs of SV viewed down the icosahedral twofold axis of symmetry (A) and the central section view through the 3D density map (B). The map was generated from individual 2D projections, which were manually selected from the digital micrographs of a negatively stained sample.

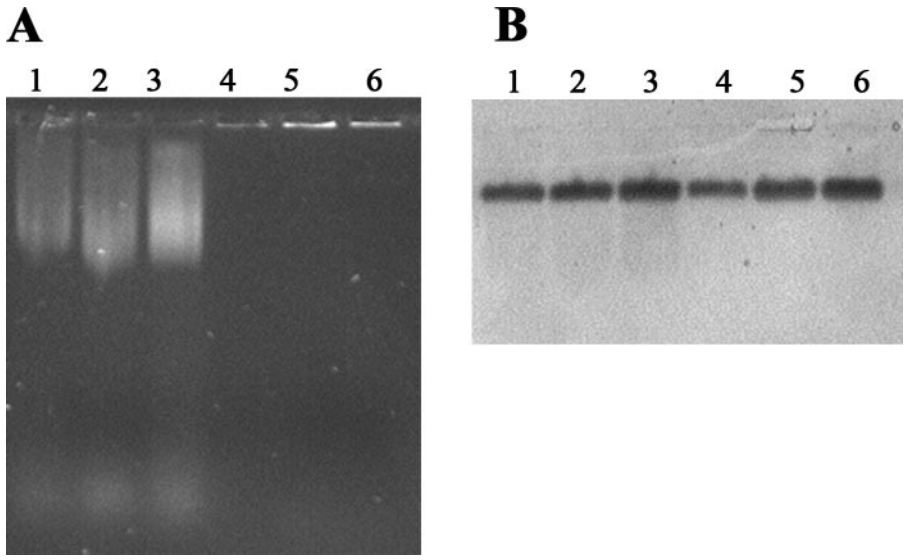

FIG. 3. Native agarose gel electrophoresis of rSV VLPs, followed by ethidium bromide staining. (A) Lanes 1 to 3, purified rSV VLPs (1 μg, 2 μg, and 3 μg, respectively); lanes 4 to 6, same as lanes 1 to 3, but samples were treated with RNase. (B) The same gel was dried and stained with Coomassie brilliant blue R-250.

This was rather surprising, as we saw mostly empty particles under the electron microscope (Fig. 1B). First-strand cDNA synthesis of the RNA isolated from the VLPs with murine leukemia virus reverse transcriptase and a capsid protein primer did not produce a PCR product, suggesting that the RNA is of cellular origin (data not shown). Interestingly, treatment of the VLPs with RNase resulted in complete degradation of RNA, indicating that the RNA was bound on the exterior surface of the rSV capsids rather than in particles encapsidating the RNA (Fig. 3A). It is also possible that the trace amounts of cellular RNA packaged into a small number of full particles could not be detected by ethidium bromide staining.

Trypsin digestion and MALDI-TOF analysis of rSV VLPs and soluble CP. Purified rSV particles were incubated with an equal volume of trypsin in serial twofold dilutions, beginning with the highest concentration of 500 μg/ml, for 30 min at 37°C. Two predominant cleavage products were observed on SDS-PAGE (Fig. 4A). MALDI-TOF analysis of the trypsin-treated VLPs revealed the mean molecular masses of these two fragments to be 26.1 and 31.7 kDa (Fig. 4B and C). To determine the exact sites of trypsinization, The VLPs were digested with trypsin, the proteolytic fragments were separated by gel electrophoresis, and the bands were transferred onto a PVDF membrane for N-terminal sequencing. Sequencing analysis of the first 10 amino acids of the 26.1-kDa cleavage product showed that the specific cleavage occurred at residue Arg307 of the rSV capsid protein (Fig. 5). Further analysis of the mass spectral data by using the proteomics tool at http://prospector.ucsf.edu/ucsfhtml4.0/msdigest.htm suggested that the 26.1-kDa band corresponds to residues 308 to 544. The last four residues from the C terminus (residue 548) could have been cleaved prior to or after the cleavage at residue 307. For unknown reasons, N-terminal sequencing of the 31.7-kDa band did not give conclusive results. However, the analysis using the proteomics tool suggested that the 31.7-kDa band might have resulted from trypsin cleavage at residue Arg292, and it corresponds to residues 1 to 292, encompassing the S domain and partial P domain. Assuming that the latter result was correct, it explains the difficulties in obtaining the N-terminal sequence of the 31.7-kDa fragment, perhaps due to possible N-terminal modifications. Interestingly, both these cleavage sites, Arg292 and Arg307, are located in and around the 20-aa insertion in the P2 domain. Even though the proteomics tool suggested that the 29.3-kDa peak found in the MALDI-TOF spectra (Fig. 4C) of the trypsin-digested soluble rSV coat protein corresponds to either residues 95 to 358 or 188 to 452, we did not further characterize this peak, as the corresponding band was not seen in SDS-PAGE or Western blot analysis.

To determine whether the 26.1- and 31.7-kDa bands were the result of trypsinization of intact VLPs or due to free subunits resulting from the disassembled capsids, SDS-PAGE and Western blot analysis of the peak fractions of the trypsin (62.5 μg/ml)-digested VLPs separated through sucrose gradients were performed. The fractions from the top of the gradient resulted in a single (26.1-kDa) band, whereas the fractions from the middle of the gradients showed both the 26.1-kDa and 31.7-kDa bands (Fig. 6A and B). Observation of both fractions by EM revealed the presence of VLPs only in the middle fractions (Fig. 6C). This clearly implies that the two (31.7-kDa and 26.1-kDa) bands are the result of trypsin digestion of the VLPs. Interestingly, the VLPs remain intact in sucrose for up to 72 h after undergoing trypsinization. On the other hand, trypsin digestion of the soluble rSV protein obtained by incubating VLPs in Tris buffer (pH 8.9) resulted in only the 26.1-kDa band at a lower concentration of trypsin (Fig. 7A and B). However, at a higher concentration of trypsin, the 26.1-kDa band was further cleaved to smaller peptides (data not shown).

Conservation of trypsin cleavage sites in human NoVs. Sequence alignment of these capsid proteins from various strains of NoVs suggested that approximately 48% of the amino acids in the S domain are conserved whereas fewer than 10% of the

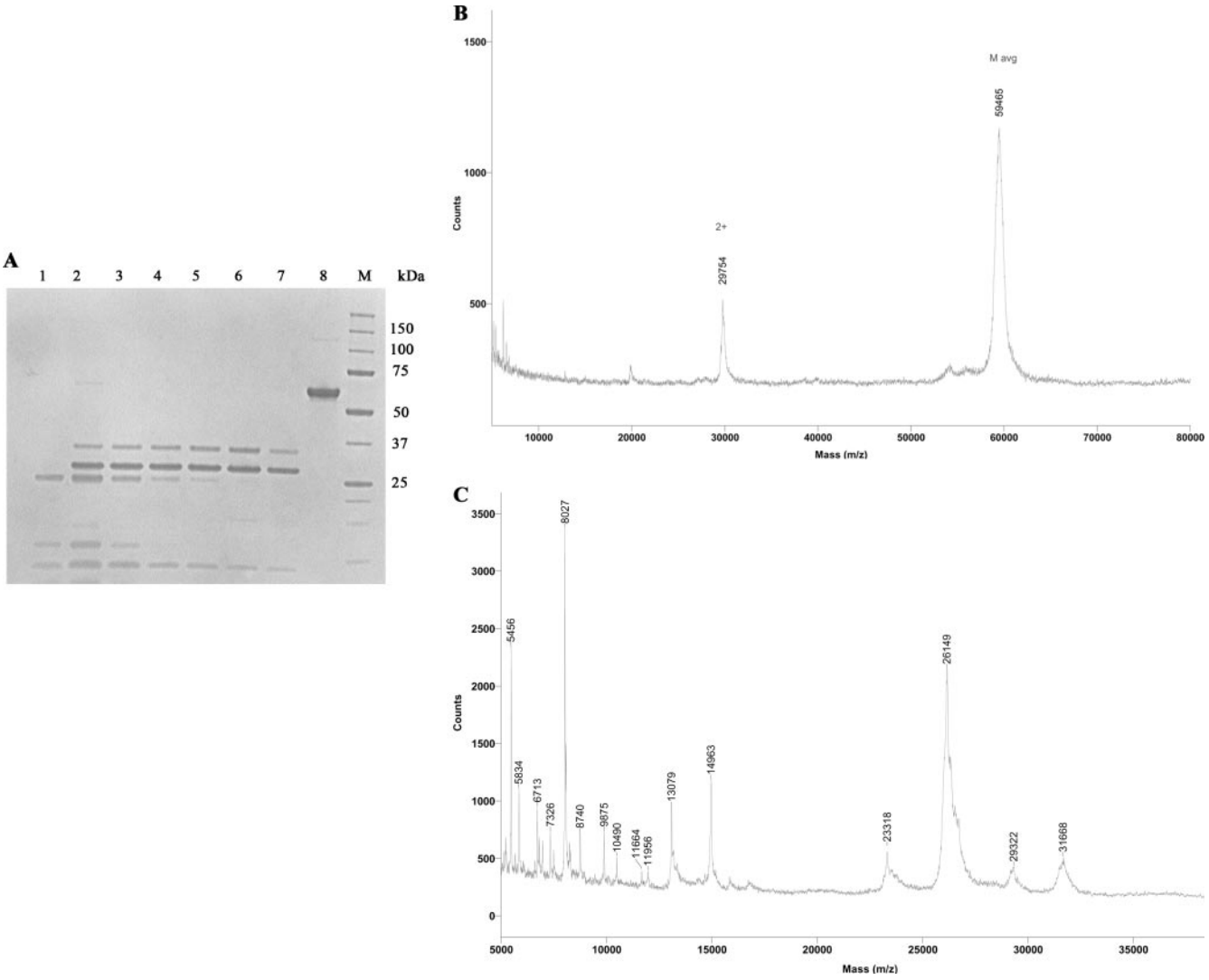

FIG. 4. SDS-PAGE and MALDI-TOF analysis of trypsin- or buffer-treated rSV particles. rSV particles were incubated with decreasing concentrations of trypsin for 30 min at 37°C and then electrophoresed on 4 to 12% bis-Tris gels. Bands were visualized by staining with Simple blue. (A) Lane 1, trypsin alone (250 μg/ml); lanes 2 to 7, rSV incubated with an equal volume of trypsin at 500 μg/ml (lane 2), 250 μg/ml (lane 3), 125 μg/ml (lane 4), 62.5 μg/ml (lane 5), 31.2 μg/ml (lane 6), and 15.6 μg/ml (lane 7); lane 8, buffer-treated rSV particles; lane M, protein molecular mass marker. The arrow indicates the trypsin band. (B and C) MALDI-TOF analysis of buffer-treated (B) and trypsin (62.5 μg/ml)-treated (C) rSV particles.

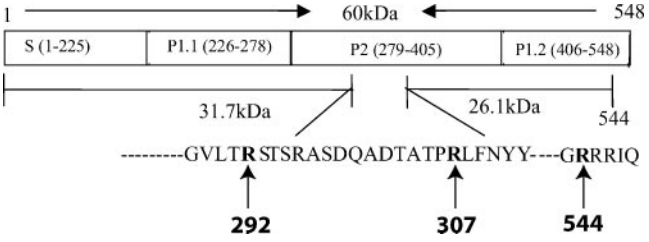

FIG. 5. Schematic diagram showing the SV residues corresponding to different structural domains, trypsin digestion fragments, and the sequence/location of trypsin cleavage sites. The arrows indicate amino acids 292, 307, and 544, where trypsin specific cleavage occurs in the assembled form of the rSV capsids.

amino acids are conserved in the P domain. The capsid protein of SV has 548 amino acid residues, whereas NV CP is composed of 530 amino acids. Alignment of these sequences revealed that the extra 18 aa present in the SV capsid protein resulted in a large insertion in the P2 domain (Fig. 8). Prediction of trypsin cleavage sites in the amino acid sequence of SV coat protein by using a web-based tool (http://ca.expasy.org/tools/peptidecutter/) suggested that there are 35 trypsin cleavage sites in the SV sequence, compared to 25 in the NV capsid protein. Of these 25 sites, only 3 trypsin cleavage sites are present in the P2 domain (aa 278 to 405) of NV, whereas 12 of the 35 potential sites are present in the P2 domain of the SV capsid protein. These 12 trypsin cleavage sites are conserved among all members of GII.3. In addition, the arginine/lysine residue at position 287 (P2 domain) is conserved in all human NoVs sequenced to date (Fig. 8). How-

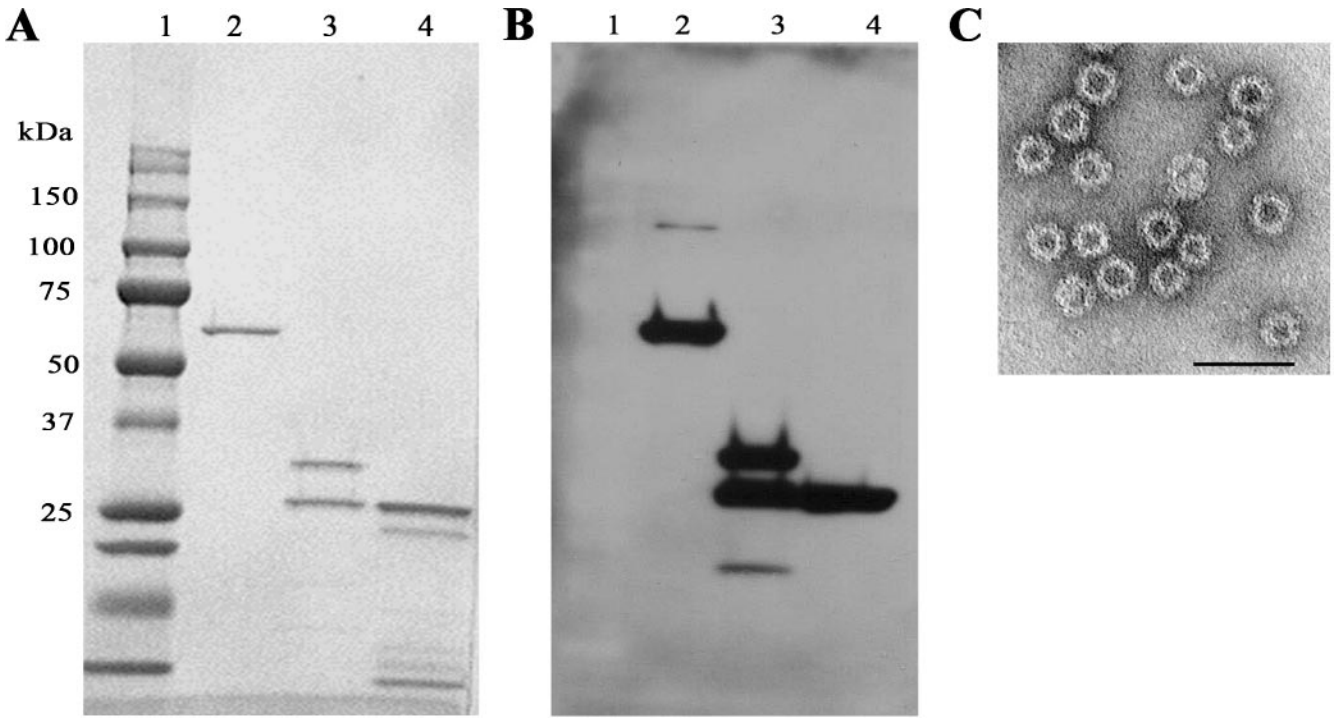

FIG. 6. SDS-PAGE, Western analysis, and electron microscopy characterization of sucrose gradient fractions of buffer-treated and trypsin (62.5 μg/ml)-treated rSV particle. (A) Lane 1, protein molecular mass marker; lane 2, buffer-treated rSV particles; lane 3, trypsin-treated rSV particles obtained from the center of the gradient; lane 4, trypsin-treated rSV protein obtained from the top of the gradient. (B) Western blot of the samples in panel A. (C) Electron micrographs of the trypsin-treated and gradient-purified rSV particles. Bar, ~100 nm.

ever, based on the modeling studies, this residue does not appear to be accessible for trypsinization in the assembled form of the coat protein.

Homology modeling of the Sinsiro virus capsid protein and mapping of trypsin cleavage sites. A structural model of Sinsiro virus capsid protein was built using the Norwalk virus capsid protein as the structural template, as described in Materials and Methods section. The resulting model is nearly identical to that of Norwalk virus coat protein, with the exception of a 20-aa insertion (residues 297 to 316) in the P2 domain of the Sinsiro virus coat protein. This insertion forms a surface-exposed loop in the assembled form of the coat protein (Fig. 9). Furthermore, the two trypsin cleavage sites are either part of this loop (Arg307) or four residues upstream of the insertion (Arg292), and these residues are surface accessible, consistent with the results from trypsinization experiments. The third site (Arg544) at the C terminus was also found to be surface exposed. Interestingly, in addition to K227, a conserved trypsin cleavage site in the hinge region of NV, three potential trypsinization sites (K289, R291, and K391) in the P2 domain of NV do not appear to be surface accessible in the assembled (capsid) form of the particles.

DISCUSSION

Expression of rSV capsid protein in insect cells resulted in spontaneous formation of VLPs, which are morphologically similar to other NoV capsids. Examination of the purified VLPs under the transmission electron microscope revealed the presence of empty as well as a few full capsids. However, the ratio of empty to full capsids differed from one preparation to another. Even though the majority of the VLPs appeared to be empty under TEM, ethidium bromide staining of VLPs on native agarose gels indicated that there is RNA associated with the particles. However, RNase treatment of VLPs led to complete dissociation/degradation of the RNA, suggesting that the RNA is bound on the external surface of the VLPs (Fig. 3). This perhaps is made possible by the presence of clusters of positively charged amino acids exposed on the surface (Fig. 9). However, it is also possible that the trace amounts of cellular RNA packaged into a very few full particles could not be detected by ethidium bromide staining. In addition, isolation of RNA associated with the VLPs followed by reverse transcription-PCR analysis showed that the RNA does not contain the viral message, and hence it might be of cellular origin.

The results obtained from in vitro trypsin digestion of the intact VLPs followed by N-terminal sequencing and mass spectrometry analysis suggested that the trypsin cleavage sites are located at amino acid residues Arg292, Arg307, and Arg544. Interestingly, two of these residues (Arg292 and Arg307) are located in and around the large insertion of 20 aa in the P2 domain, while the third site, Arg544, is located near the C terminus. Homology modeling studies clearly indicated that this insertion is unstructured and surface exposed, thus facilitating the ease of trypsinization at these three sites (Fig. 9). There is another conserved basic residue (R296) in this loop, which has potential to be trypsinized. However, further proteolysis at residues R292 and R307 on either side of R296 could release the short peptides of residues 293 to 296 and 297 to

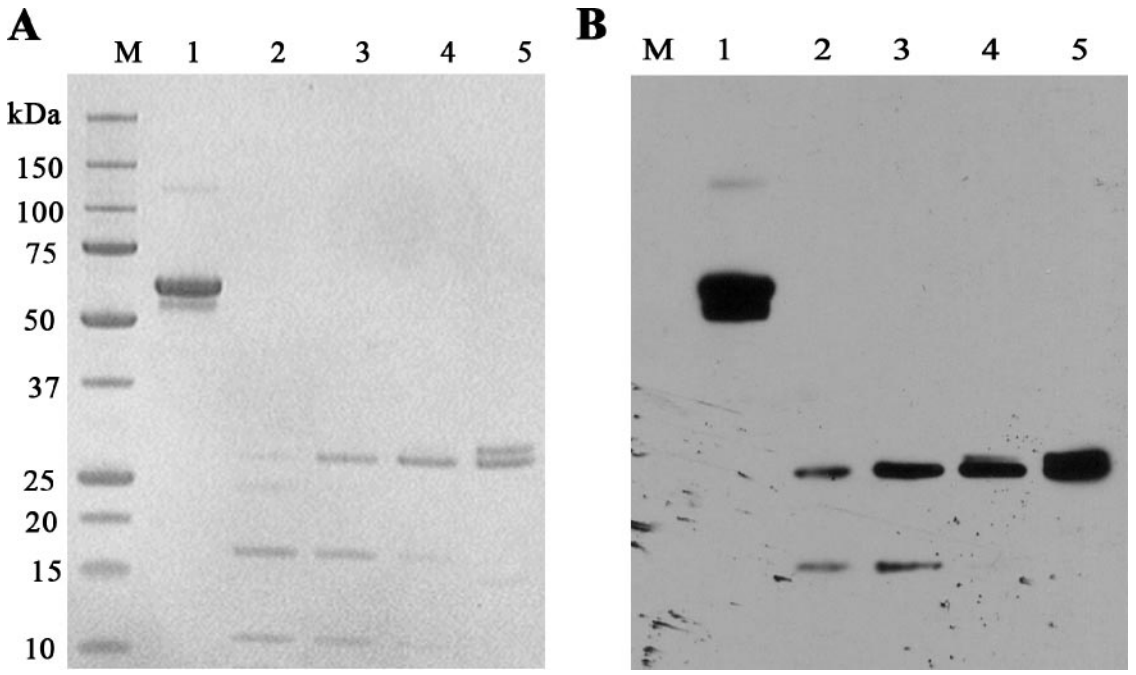

FIG. 7. SDS-PAGE and Western blot analysis of trypsin- and buffer-treated rSV solubilized protein. (A) Lane M, protein molecular mass marker; lane 1, buffer-treated rSV solubilized protein; lanes 2 to 5, rSV solubilized protein incubated with an equal volume of trypsin at 125 μg/ml (lane 2), 62.5 μg/ml (lane 3), 31.2 μg/ml (lane 4), and 15.6 μg/ml (lane 5). (B) Western blot corresponding to the samples in panel A.

306. Hence, the cleavage at residue R296 may not have a significant impact. Remarkably, the large insertion of 20 aa (relative to NV) appears to be a characteristic of the GII.3 and GII.6 NoVs along with the conservation of all three trypsin cleavage sites, implying a potential biological role for this insertion.

Earlier studies by Hardy et al. suggested that NV particles are resistant to trypsinzation (18). They have also shown that the free coat protein subunits undergo trypsinization, thereby releasing the intact P domain. Our results are in good agreement with those of Hardy et al., as the GI.1 NoVs (e.g., Norwalk virus) lack the large surface insertion as seen in the GII.3 viruses (e.g., Sinsiro virus) and none of other basic residues are available for trypsinization in the particle form, except for the cluster of arginines near the C terminus. Hence, the group I NoVs may not undergo trypsinization in the assembled form to release the intact P domain. However, the above results do not support the recent findings reported by Tan et al. (36), who suggested that the NV (GI) and VA387 (GII.4) particles, both of which lack the long insertion (only a 12-aa insertion in the case of VA387) comprised of basic amino acids, undergo partial trypsin digestion, thereby releasing the intact P domains. This is a rather surprising finding, as Lys227 in NV or its counterparts near the hinge regions of other NoVs, which need to be proteolysed to release the P domain, are in fact buried and would be inaccessible for trypsinization in all the intact norovirus capsids. This site would become accessible for trypsinization only in the free and soluble form of the CP

```
Norwalk        (G1_1) 291 RGTSNGTVIN--------------------LTELDG...... SARGRLGLRR 530
Msham-Gbr95    (G2_2) 287 KGEVTAHLHDNDH------------LNNVTITNLNG...... GRRRVQ---- 542
Hilingd-GBR00  (G2_5) 287 RGKVTGQFPNEQN------------MWNLEITNLNG...... GRRRFQ---- 540
Erfurt-DEU01   (G2_10)287 RGKVTQQVQDEHRG----------THWNMTVTNLNG...... GRRRMQ---- 548
Hawaii-USA91   (G2_1) 287 RGRINAQVPDDHH------------QWNLQVTNTNG...... GRRRVQ---- 535
Amstdam-NLD99  (G2_8) 287 RGTLQTR-----------LADQPNYTYQVHLENLDG...... GRRRVQ---- 537
VABeach-USA01  (G2_9) 287 KGTLQAE-----------VPG-QHQLYQLQLTNLDG...... GRRRIQ---- 537
Leeds-GBR00    (G2_7) 287 KGEVIAK-----------NGDVRSYRMDMEITNTDG...... GRRRVQ---- 540
Toronto-CAN93  (G2_3) 287 RGTLTRSTSRASDQADTPTPRLFNYYWHIQLDNLNG...... GRRRIQ---- 548
Sinsiro        (G2_3) 287 RGVLTRSTSRASDQADTATPRLFNYYWHVQLDNLNG...... GRRRIQ---- 548
Seacrof-GBR00  (G2_6) 286 RGTLISQTARAADSTDSPQ-RARNHPLHVQVKNLDG...... GRRRAQ---- 550
Bristol-GBR93  (G2_4) 287 RGDVTHIAG--------------SHDYTMNLASQNW...... GRRRAL---- 539
VA387          (G2_4) 287 RGDVTHIAG--------------SHDYIMNLASQNW...... GRRRAL---- 539
```

FIG. 8. Sequence alignment of the P2 domains of various strains of NoVs belonging to different genogroups, where a large insertion occurs in Sinsiro virus. The boxed sequence represents the 20-amino-acid insertion in the GII.3 and GII.6 NoVs with respect to Norwalk virus (GI.1). The genogroup classification of each strain is shown in parentheses. The start and end residue numbers corresponding to each sequence are listed. Arginine residues that undergo trypsinization in SV are underlined.

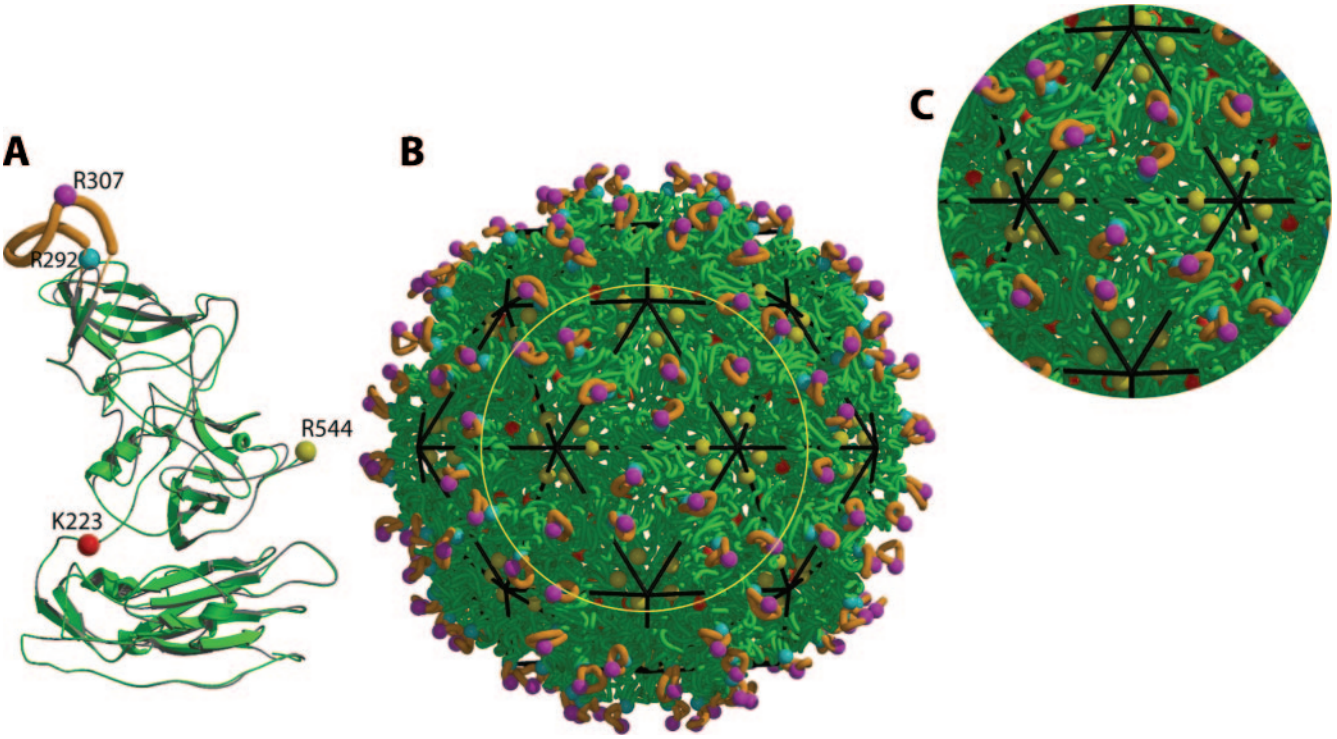

FIG. 9. Comparative model of the SV capsid, generated using NV as the structural model. (A) Ribbon diagram showing the tertiary fold of the SV coat protein subunit (green), which is superimposed on the subunit of Norwalk virus (thin gray tube). The 20-aa insertion is highlighted in orange. Locations of the SV residues that undergo (R292, R307, R544) or have the potential to but did not undergo (K223) trypsin digestion in the particle form are shown as spheres, and the corresponding residue numbers are listed. The residues shown in gray and black spheres are those of the Norwalk virus coat protein which are not accessible for trypsinization in the particle form. (B) A complete capsid model of SV, showing the relative dispositions and exposures of the residues. (C) Zoom-in view of the highlighted (circular) region of the capsid in panel B.

subunits or at minimum in the disassembled and/or partially assembled forms of capsids.

Sinsiro virus has 12 trypsin cleavage sites (Arg287, Arg292, Arg296, Arg307, Arg341, Lys343, Arg351, Arg358, Lys363, Arg370, Lys374, and Arg394) in the P2 domain. Based on the trypsin digestion experiments and modeling studies, the trypsin cleavage sites at Arg292 and Arg307 are accessible to trypsinization even in the assembled VLPs. In contrast, there are only three potential trypsin cleavage sites (Lys289, Arg291, and Lys391) present in the P2 domain of NV. Based on modeling studies, all these sites appeared to be buried, except for residue Lys391, which is partially exposed. However, none of these sites have been reported to be accessible for trypsin digestion in the assembled form of Norwalk virus (18, 36).

Remarkably, TEM characterization of the trypsin-treated rSV particles revealed that the VLPs remain intact even after trypsin digestion (Fig. 6C). The cleaved fragments remain associated with the rest of capsid, perhaps due to close interactions between the P domains up to 72 h after trypsin treatment. Trypsin digestion of the soluble capsid protein of SV obtained by disassembly of VLPs showed a single 26.1-kDa fragment (aa 308 to 544) of the P domain, which is resistant to further proteolysis at low concentrations of trypsin (Fig. 6). This clearly shows that Arg307 is accessible for trypsinization in both the assembled and unassembled forms of the Sinsiro virus coat protein subunits. However, higher concentrations of trypsin led to complete degradation of SV capsid protein (data not shown). We surmise that the 31.7-kDa fragment in its unassembled form is digested into smaller fragments even at low concentrations of trypsin.

Earlier studies suggested that the hypervariable region of the P2 domain (aa 300 to 405) of NV is the main region where immune response-driven mutations are localized (26). In addition, the P2 domain also contains the determinants for strain specificity (29). Moreover, monoclonal antibodies that recognize residues 300 to 384 in the P2 domain readily inhibit the binding of NV capsids to cells (39). Several studies using recombinant peptides and domain swaps have shown that the neutralization epitopes in feline calicivirus also map to the hypervariable region in the P2 domain (37). Recently, Lochridge et al. further narrowed down the antigenic epitopes to amino acids 291 to 293 and 313 to 322 in the P2 domains of NV and Snow Mountain virus, which are the reference strains of GI.1 and GII.2, respectively (23). The linear epitope composed of amino acids 313 to 322 in Snow Mountain virus, which has been suggested to be responsible for the host cell interactions, is conserved among all the NoVs (23). Remarkably, the corresponding residues 325 to 334 in SV remain contiguous even after trypsin digestion, suggesting that the trypsin-treated particles, in principle, are capable of binding to cells.

For viruses that replicate on mucosal surfaces and particularly in the gastrointestinal tract, proteolytic cleavage of outer capsid proteins plays an important role in the replication cycle of the parent viruses. Previous studies on rotaviruses clearly

indicated that the trypsin cleavage of the outer capsid protein leads to a severalfold increase in infectivity (11). We hypothesize that the proteolytic cleavage of SV capsids at residues R292 and R307 results in less restraint on residues 325 to 334, thereby enhancing their ability to bind cells. This perhaps could be one of the reasons for greater virulence of Sinsiro virus and GII.3 NoVs in general, as well as GII.6 NoVs. In addition, the proteolytic cleavage may also promote the viral infection by inhibiting the binding of neutralizing antibodies against the native virus to the "nicked" virus.

ACKNOWLEDGMENTS

We thank Milena Iacobelli-Martinez and Ajay Vashisht for carefully going through the manuscript and providing helpful suggestions. We also acknowledge Catherine Hsu for the help and advice in generating baculovirus constructs.

The work reported in this paper was supported by the USAMRIID under contract no. W81XWH-04-2-0027 to V.S.R. and by NIH Research Resource: Multiscale Modeling Tools for Structural Biology (MMTSB), RR12255.

REFERENCES

1. **Ando, T., J. S. Noel, and R. L. Fankhauser.** 2000. Genetic classification of "Norwalk-like viruses. J. Infect. Dis. **181**(Suppl. 2)**:**S336–S348.
2. **Atmar, R. L., and M. K. Estes.** 2001. Diagnosis of noncultivatable gastroenteritis viruses, the human caliciviruses. Clin. Microbiol. Rev. **14:**15–37.
3. **Ausar, S. F., T. R. Foubert, M. H. Hudson, T. S. Vedvick, and C. R. Middaugh.** 2006. Conformational stability and disassembly of Norwalk virus-like particles. Effect of pH and temperature. J. Biol. Chem. **281:**19478–19488.
4. **Baker, T. S., J. Drak, and M. Bina.** 1988. Reconstruction of the three-dimensional structure of simian virus 40 and visualization of the chromatin core. Proc. Natl. Acad. Sci. USA. **85:**422–426.
5. **Baker, T. S., W. W. Newcomb, N. H. Olson, L. M. Cowsert, C. Olson, and J. C. Brown.** 1991. Structures of bovine and human papillomaviruses. Analysis by cryoelectron microscopy and three-dimensional image reconstruction. Biophys. J. **60:**1445–1456.
6. **Baker, T. S., N. H. Olson, and S. D. Fuller.** 1999. Adding the third dimension to virus life cycles: three-dimensional reconstruction of icosahedral viruses from cryo-electron micrographs. Microbiol. Mol. Biol. Rev. **63:**862–922.
7. **Bertolotti-Ciarlet, A., L. J. White, R. Chen, B. V. Prasad, and M. K. Estes.** 2002. Structural requirements for the assembly of Norwalk virus-like particles. J. Virol. **76:**4044–4055.
8. **Carrascosa, J. L., and A. C. Steven.** 1978. A procedure for evaluaton of significant structural differences between related arrays of protein molecules. Micron **9:**199–206.
9. **Chakravarty, S., A. M. Hutson, M. K. Estes, and B. V. Prasad.** 2005. Evolutionary trace residues in noroviruses: importance in receptor binding, antigenicity, virion assembly, and strain diversity. J. Virol. **79:**554–568.
10. **Chen, R., J. D. Neill, M. K. Estes, and B. V. Prasad.** 2006. X-ray structure of a native calicivirus: structural insights into antigenic diversity and host specificity. Proc. Natl. Acad. Sci. USA. **103:**8048–8053.
11. **Crawford, S. E., S. K. Mukherjee, M. K. Estes, J. A. Lawton, A. L. Shaw, R. F. Ramig, and B. V. Prasad.** 2001. Trypsin cleavage stabilizes the rotavirus VP4 spike. J. Virol. **75:**6052–6061.
12. **Fankhauser, R. L., S. S. Monroe, J. S. Noel, C. D. Humphrey, J. S. Bresee, U. D. Parashar, T. Ando, and R. I. Glass.** 2002. Epidemiologic and molecular trends of"Norwalk-like viruses" associated with outbreaks of gastroenteritis in the United States. J. Infect. Dis. **186:**1–7.
13. **Fankhauser, R. L., J. S. Noel, S. S. Monroe, T. Ando, and R. I. Glass.** 1998. Molecular epidemiology of "Norwalk-like viruses" in outbreaks of gastroenteritis in the United States. J. Infect. Dis. **178:**1571–1578.
14. **Gallimore, C. I., D. Lewis, C. Taylor, A. Cant, A. Gennery, and J. J. Gray.** 2004. Chronic excretion of a norovirus in a child with cartilage hair hypoplasia (CHH). J. Clin. Virol. **30:**196–204.
15. **Glass, P. J., L. J. White, J. M. Ball, I. Leparc-Goffart, M. E. Hardy, and M. K. Estes.** 2000. Norwalk virus open reading frame 3 encodes a minor structural protein. J. Virol. **74:**6581–6591.
16. **Green, K. Y., A. Z. Kapikian, J. Valdesuso, S. Sosnovtsev, J. J. Treanor, and J. F. Lew.** 1997. Expression and self-assembly of recombinant capsid protein from the antigenically distinct Hawaii human calicivirus. J. Clin. Microbiol. **35:**1909–1914.
17. **Green, S. M., P. R. Lambden, E. O. Caul, and I. N. Clarke.** 1997. Capsid sequence diversity in small round structured viruses from recent UK outbreaks of gastroenteritis. J. Med. Virol. **52:**14–19.
18. **Hardy, M. E., L. J. White, J. M. Ball, and M. K. Estes.** 1995. Specific proteolytic cleavage of recombinant Norwalk virus capsid protein. J. Virol. **69:**1693–1698.
19. **Hirakata, Y., K. Arisawa, O. Nishio, and O. Nakagomi.** 2005. Multiprefectural spread of gastroenteritis outbreaks attributable to a single genogroup II norovirus strain from a tourist restaurant in Nagasaki, Japan. J. Clin. Microbiol. **43:**1093–1098.
20. **Jiang, X., M. Wang, D. Y. Graham, and M. K. Estes.** 1992. Expression, self-assembly, and antigenicity of the Norwalk virus capsid protein. J. Virol. **66:**6527–6532.
21. **Koopmans, M., J. Vinje, M. de Wit, I. Leenen, W. van der Poel, and Y. van Duynhoven.** 2000. Molecular epidemiology of human enteric caliciviruses in The Netherlands. J. Infect. Dis. **181**(Suppl. 2)**:**S262–S269.
22. **Lau, C. S., D. A. Wong, L. K. Tong, J. Y. Lo, A. M. Ma, P. K. Cheng, and W. W. Lim.** 2004. High rate and changing molecular epidemiology pattern of norovirus infections in sporadic cases and outbreaks of gastroenteritis in Hong Kong. J. Med. Virol. **73:**113–117.
23. **Lochridge, V. P., K. L. Jutila, J. W. Graff, and M. E. Hardy.** 2005. Epitopes in the P2 domain of norovirus VP1 recognized by monoclonal antibodies that block cell interactions. J. Gen. Virol. **86:**2799–2806.
24. **Lopman, B., H. Vennema, E. Kohli, P. Pothier, A. Sanchez, A. Negredo, J. Buesa, E. Schreier, M. Reacher, D. Brown, J. Gray, M. Iturriza, C. Gallimore, B. Bottiger, K. O. Hedlund, M. Torven, C. H. von Bonsdorff, L. Maunula, M. Poljsak-Prijatelj, J. Zimsek, G. Reuter, G. Szucs, B. Melegh, L. Svennson, Y. van Duijnhoven, and M. Koopmans.** 2004. Increase in viral gastroenteritis outbreaks in Europe and epidemic spread of new norovirus variant. Lancet **363:**682–688.
25. **Meakins, S. M., G. K. Adak, B. A. Lopman, and S. J. O'Brien.** 2003. General outbreaks of infectious intestinal disease (IID) in hospitals, England and Wales, 1992–2000. J. Hosp. Infect **53:**1–5.
26. **Nilsson, M., K. O. Hedlund, M. Thorhagen, G. Larson, K. Johansen, A. Ekspong, and L. Svensson.** 2003. Evolution of human calicivirus RNA in vivo: accumulation of mutations in the protruding P2 domain of the capsid leads to structural changes and possibly a new phenotype. J. Virol. **77:**13117–13124.
27. **Phan, T. G., F. Yagyu, V. Kozlov, A. Kozlov, S. Okitsu, W. E. Muller, and H. Ushijima.** 2006. Viral gastroenteritis and genetic characterization of recombinant norovirus circulating in Eastern Russia. Clin. Lab. **52:**247–253.
28. **Pletneva, M. A., S. V. Sosnovtsev, and K. Y. Green.** 2001. The genome of Hawaii virus and its relationship with other members of the caliciviridae. Virus Genes **23:**5–16.
29. **Prasad, B. V., M. E. Hardy, T. Dokland, J. Bella, M. G. Rossmann, and M. K. Estes.** 1999. X-ray crystallographic structure of the Norwalk virus capsid. Science **286:**287–290.
30. **Reuter, G., H. Vennema, M. Koopmans, and G. Szucs.** 2006. Epidemic spread of recombinant noroviruses with four capsid types in Hungary. J. Clin. Virol. **35:**84–88.
31. **Rohayem, J., J. Munch, and A. Rethwilm.** 2005. Evidence of recombination in the norovirus capsid gene. J. Virol. **79:**4977–4990.
32. **Sali, A., and T. L. Blundell.** 1993. Comparative protein modelling by satisfaction of spatial restraints. J. Mol. Biol. **234:**779–815.
33. **Schneemann, A., R. Dasgupta, J. E. Johnson, and R. R. Rueckert.** 1993. Use of recombinant baculoviruses in synthesis of morphologically distinct virus-like particles of flock house virus, a nodavirus. J. Virol. **67:**2756–2763.
34. **Shepherd, C. M., I. A. Borelli, G. Lander, P. Natarajan, V. Siddavanahalli, C. Bajaj, J. E. Johnson, C. L. Brooks III, and V. S. Reddy.** 2006. VIPERdb: a relational database for structural virology. Nucleic Acids Res. **34:**D386–D389.
35. **Tan, M., P. Huang, J. Meller, W. Zhong, T. Farkas, and X. Jiang.** 2003. Mutations within the P2 domain of norovirus capsid affect binding to human histo-blood group antigens: evidence for a binding pocket. J. Virol. **77:** 12562–12571.
36. **Tan, M., J. Meller, and X. Jiang.** 2006. C-terminal arginine cluster is essential for receptor binding of norovirus capsid protein. J. Virol. **80:**7322–7331.
37. **Tohya, Y., N. Yokoyama, K. Maeda, Y. Kawaguchi, and T. Mikami.** 1997. Mapping of antigenic sites involved in neutralization on the capsid protein of feline calicivirus. J. Gen. Virol. **78:**303–305.
38. **Vinje, J., J. Green, D. C. Lewis, C. I. Gallimore, D. W. Brown, and M. P. Koopmans.** 2000. Genetic polymorphism across regions of the three open reading frames of "Norwalk-like viruses." Arch. Virol. **145:**223–241.
39. **White, L. J., J. M. Ball, M. E. Hardy, T. N. Tanaka, N. Kitamoto, and M. K. Estes.** 1996. Attachment and entry of recombinant Norwalk virus capsids to cultured human and animal cell lines. J. Virol. **70:**6589–6597.
40. **White, L. J., M. E. Hardy, and M. K. Estes.** 1997. Biochemical characterization of a smaller form of recombinant Norwalk virus capsids assembled in insect cells. J. Virol. **71:**8066–8072.
41. **Zheng, D. P., T. Ando, R. L. Fankhauser, R. S. Beard, R. I. Glass, and S. S. Monroe.** 2006. Norovirus classification and proposed strain nomenclature. Virology **346:**312–323.
42. **Zintz, C., K. Bok, E. Parada, M. Barnes-Eley, T. Berke, M. A. Staat, P. Azimi, X. Jiang, and D. O. Matson.** 2005. Prevalence and genetic characterization of caliciviruses among children hospitalized for acute gastroenteritis in the United States. Infect. Genet. Evol. **5:**281–290.